nature communications

Review article

https://doi.org/10.1038/s41467-025-62063-8

Nanozymes expanding the boundaries of biocatalysis

Received: 4 September 2024

Accepted: 9 July 2025

Published online: 24 July 2025

Check for updates

Ruofei Zhang [1], Xiyun Yan [1,2], Lizeng Gao [1,2] ✉ & Kelong Fan [1,2] ✉

Biocatalysis is fundamental to biological processes and sustainable applications. Over time, the understanding of biocatalysis has evolved considerably. Initially, protein enzymes were recognized as the primary biocatalysts due to their high catalytic efficiency under mild conditions. The discovery of ribozymes expanded the scope of biocatalysts to include nucleic acids and the development of synthetic or semisynthetic artificial enzymes sought to overcome the limitations of natural enzymes. The emergence of nanozymes, nanomaterials with intrinsic biocatalytic activity, has further broadened this field. Nanozymes possess abundant active sites, multiple active phases, and nanostructures that maintain stability even under extreme conditions, along with unique physicochemical properties. These attributes enable nanozymes to perform efficient biocatalysis in diverse forms and under a wide range of conditions. The discovery of natural biogenic nanozymes, such as magnetosomes, ferritin iron cores, and amyloid protein assemblies, underscores their potential physiological functions and roles in disease pathogenesis. This review explores the distinct properties and catalytic mechanisms of nanozymes, elucidates their structure-activity relationships, and discusses their transformative impact on biocatalysis, highlighting their potential to reshape fundamental concepts and practical applications in the field.

Biocatalysis involves the use of biocatalysts, such as enzymes or enzyme mimics, to accelerate biochemical reactions in biological systems or biomimetic environments. For millennia, humans have harnessed enzymes, initially without understanding their nature, in processes like brewing and cheese-making[1]. Diastase was discovered in 1833 from malt extract[2], followed by the identification of other hydrolytic enzymes, including pepsin, trypsin, and invertase[3,4]. In 1835, the concept of catalysis was introduced to describe reactions accelerated by substances that remain unchanged after the reaction[5]. The hydrolysis of starch by diastase was hypothesized to be a catalytic reaction. The term "enzyme" was coined in 1877, derived from the Greek word ενζυμον meaning "in leaven," reflecting the early association of biocatalysis with fermentation studies[6].

In 1860, Louis Pasteur observed yeast activity in alcoholic fermentation through a microscope and proposed that fermentation occurred within living yeast and was driven by a vital force called "ferments"[7]. This "vitalism" notion was disproved in 1897 when Eduard Buchner demonstrated cell-free fermentation using yeast extracts, proving that enzymes can independently drive alcoholic fermentation[8]. In 1926, the enzyme urease was crystallized by James Batcheller Sumner[9], soon followed by the crystallization of pepsin, trypsin, chymotrypsin, and catalase, cementing the conclusion that pure proteins can be enzymes[10]. The discovery of ribozyme, RNA with catalytic properties, in the 1980s expanded the definition of enzymes to include nucleic acids[11]. This historical overview shows that biocatalysis continues to reveal its true nature and extend its boundaries over the past 200 years (Fig. 1).

Biocatalysis holds substantial value in industries such as food, textiles, pharmaceuticals, and medicine due to its high catalytic efficiency, selectivity, and compatibility with mild working conditions.

[1]State Key Laboratory of Biomacromolecules, Institute of Biophysics, Chinese Academy of Sciences, Beijing, China. [2]Nanozyme Laboratory in Zhongyuan, Henan Academy of Innovations in Medical Science, Zhengzhou, Henan, China. ✉e-mail: gaolizeng@ibp.ac.cn; fankelong@ibp.ac.cn

https://doi.org/10.1038/s41467-025-62063-8

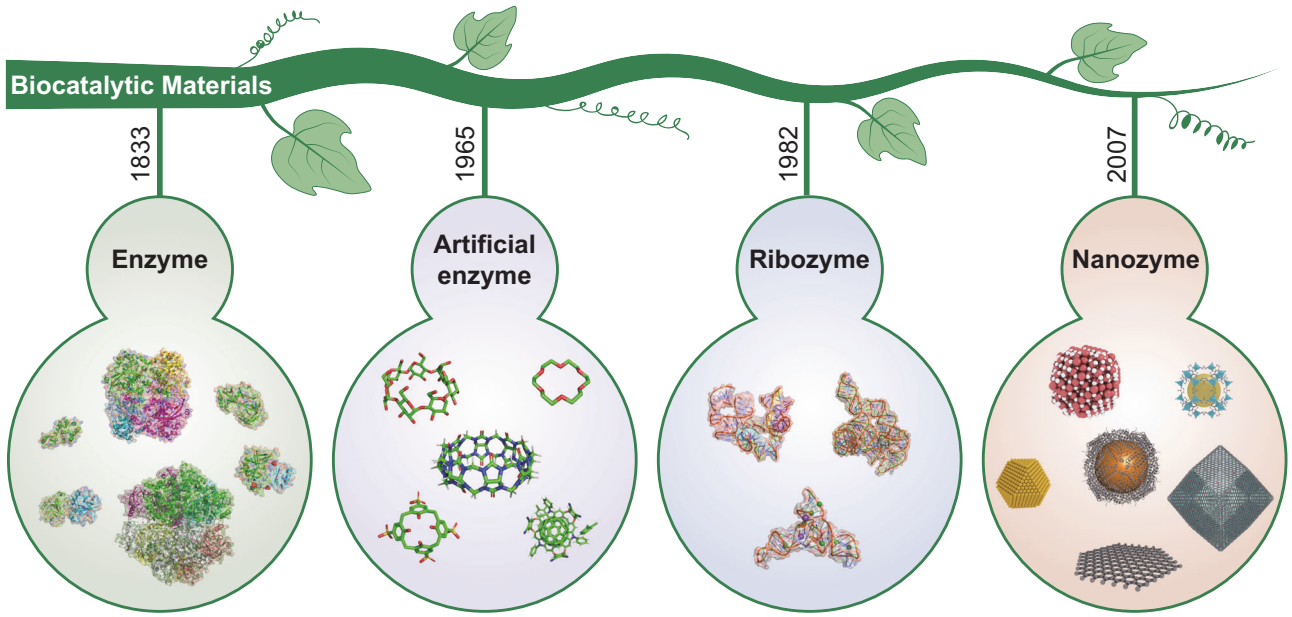

Fig. 1 | Schematic illustration of nanozymes as a class of biocatalytic materials.

Early industrial enzymes were naturally sourced from animals, plants, and microorganisms, such as alkaline protease from *Bacillus licheniformis* for detergent production[12], rennet from calves' rumen for cheese-making[13], and papain from papaya fruit for food tenderization[14]. Enzyme engineering was developed in the 1960s to address issues of high cost, poor stability, low efficiency, and limited working conditions of enzymes in industrial applications through methods including enzyme preparation, immobilization, and modification[15,16]. Enzyme engineering has promoted the application of natural enzymes, but inherent limitations like limited sources and complex production processes meant only few natural enzymes could be used for large-scale production. The advent of recombinant DNA technology in the 1970s allowed the use of genetically engineered strains to produce enzymes, reducing costs associated with natural enzyme extraction[17]. Technologies like gene mutation and directed evolution, pioneered by Frances H. Arnold, greatly improved enzyme stability, catalytic activity, and selectivity, expanding their industrial applications[18,19]. Directed evolution has also been used to develop enzymes with new-to-nature functions. For example, Frances H. Arnold evolved cytochrome P450 to catalyze carbene and nitrene transfer reactions[20,21].

Biocatalysis was initially limited to natural enzymes produced by cells until the mid-twentieth century, when the concept of artificial enzymes was proposed[22]. Artificial enzymes are synthesized using chemical or biological methods to simulate the substrate-binding and catalytic processes of natural enzymes. Various types have been developed, including synthetic enzyme mimics based on cyclodextrins, crown ethers, linear or cyclic peptides, micelles, and molecularly imprinted polymers[23,24]. In addition, semi-synthetic enzymes are produced by modifying natural proteins or enzymes with chemical methods to introduce active sites or catalytic groups[25]. DNAzymes[26] and abzymes (catalytic antibodies)[27] have further diversified the field of biocatalysis. Despite these progress, the catalytic activity of most artificial enzymes remains inferior to that of natural enzymes, and developing high-activity artificial enzymes continues to be a major focus of scientific research.

At the beginning of the twenty-first century, advancements in nanoscience deepened our understanding of microscopic matter, making nanomaterials a prominent research topic. In 2007, Fe_3O_4 nanoparticles were discovered to exhibit intrinsic catalytic activity similar to horseradish peroxidase (HRP), revealing a new nano-bio effect[28]. Since then, research on nanomaterials with biocatalytic characteristics (nanozymes) has rapidly expanded (Box 1)[29]. To date, thousands of nanomaterials, including metal oxides, noble metals, carbon materials, metal-organic frameworks, and nano-assembled biomolecules, have demonstrated biocatalytic activity (Box 2)[30]. These materials exhibit various biocatalytic activities, such as oxidoreductase-like activities, including peroxidase-like, catalase-like, oxidase-like, and superoxide dismutase-like activities[31]; hydrolase-like activities, such as phosphatase-like, protease-like, and glycosidase-like activities[32]; as well as lyase-like[33] and isomerase-like[34] activities in a few cases. Unlike traditional artificial enzymes that mimic the catalytic structures or mechanisms of natural enzymes, nanozymes have unique nanostructures and mechanisms that drive their intrinsic biocatalytic properties. Nanozymes possess multiple nanostructure-confined active sites, providing interfaces for substrate interactions and enabling diverse catalytic functions[35]. Their catalytic properties can be tailored by adjusting size and morphology[31]. Additionally, nanozymes integrate biocatalytic activity with unique nano-physicochemical properties, such as supermagnetism and photothermal effects, making them versatile and multifunctional entities[36].

The discovery of nanozymes reveals that nanomaterials are not inert in biological systems but are catalytically active. This expands biocatalysis beyond enzymes and their mimics to include nanomaterials capable of catalyzing biochemical reactions (Fig. 1). Nanozymes offer unique structural stability, designability, and multifunctionality, making them valuable in breaking through the limitations of enzymes and expanding the application of biocatalysis across various fields, such as biomedicine, environmental management, and agriculture[37–39]. Especially, preclinical results increasingly highlight their potential in catalytic medicine, with research progressing from in vitro biosensing to in vivo disease treatment for diseases like tumors, bacterial infection, neurodegenerative disorders, and stroke[40]. These advances lay a foundation for nanozymes to contribute to human health. Moreover, certain natural nanomaterials within organisms, such as magnetosomes[41], ferritin iron cores[42], and polypeptide nanoaggregates[43], have been found to perform biocatalytic functions. These discoveries deepen our understanding of biocatalysis, raising questions about whether other substances within organisms, beyond gene-coded proteins and nucleic acids, contribute to biocatalytic

BOX 1

Nanozymes as biocatalytic materials

Biocatalysts are traditionally defined as entities of biological origin that catalyze chemical reactions[229–231], typically under mild conditions (e.g., physiological temperature, pH, ionic strength, and limited substrate concentrations)[232]. Nanozymes, though mostly synthetic, inherently possess the ability to catalyze existing or new-to-nature biochemical reactions, irrespective of whether their substrates and products match those of enzymes. The development of nanozymes for reactions that enzymes cannot catalyze is important, as it could lead to the discovery of new catalytic processes with broad applications in areas where enzymes are limited. Moreover, nanozymes operate efficiently under mild, biologically compatible conditions, in contrast to conventional nanocatalysts that require high-energy inputs or concentrated substrates. This positions them as promising candidates for sustainable applications in environmental remediation, chemical synthesis, and energy production.

Traditional enzyme mimics are typically designed to replicate the common features found in the active sites of enzymes, including the ability to bind and stabilize reaction transition states, transform intermolecular reactions of reactants into (pseudo) intramolecular reactions, the presence of correctly oriented and located functional groups, and solvation properties and local pH different from those of the bulk solution[50]. In contrast, nanozymes often possess structures that differ greatly from enzymes yet remain effective in biocatalytic processes. This suggests that enzymes are not the only blueprint for catalyzing biochemical reactions and underscores the biocatalytic potential of synthetic nanostructures. Although nanozymes designed to resemble these enzymatic characteristics often exhibit enhanced biocatalytic performance, we recommend that a nanoscale perspective shall be placed on understanding the processes occurring at the active site of nanozyme during the chemical transformation of the substrate, which may share some enzyme-like properties but also may involve its unique mechanisms.

Nanozymes are characterized by their nanoscale architectures, which provide spatially confined interfaces to interact with substrates, distinguishing them from ionic catalysts (e.g., Fenton reagents) and traditional small-molecule enzyme mimics. With a high surface area-to-volume ratio and multiple active sites, nanozymes enable efficient substrate interactions, often performing apparent binding profiles in enzymatic kinetics following the Michaelis–Menten equation. However, their binding modes differ from those of enzymes. Enzymes bind substrates typically through an induced-fit mechanism at a specialized binding pocket, whereas nanozymes rely on surface-mediated interactions, including electrostatic forces (e.g., in metal-based nanozymes) or hydrophobic interactions (e.g., in carbon-based nanozymes) for substrate binding, facilitated by multiple surface features such as nanostructural motifs, defects, and functional groups[69,114]. For example, glucose oxidase binds glucose at a precise active site and mediates electron transfer from glucose to O_2 through the sequential redox cycling of its flavin cofactor ($FAD/FADH_2$)[233]. In comparison, gold (Au) nanozymes catalyze glucose oxidation by adsorbing glucose onto their surface and acting as electron transfer mediators to directly transfer electrons from glucose to O_2[234]. Although less specific than enzymatic processes, these mechanisms are effective for certain biocatalytic applications, such as pollutant degradation, biomolecule sensing, and bacterial eradication. Future nanozyme development could draw inspiration from enzymes, such as incorporating specific recognition motifs or allosteric regulation, to evolve from broad-spectrum, less specific substrate adsorption to more refined systems with tailored binding interactions, enhancing substrate specificity and reaction precision.

processes. It also prompts a consideration that nanozymes could represent some of the primordial biocatalysts, potentially functioning under extreme conditions, such as the harsh environments on early Earth, where delicate protein- and nucleic acid-based enzymes could not function[44].

Nanozymes are advancing rapidly, and our understanding of their properties and mechanisms continues to evolve. In this review, we introduce the fundamental definition of nanozymes and their distinctive characteristics, highlight their potential as biocatalytic materials in biomedical applications, and discuss the physiological and pathological effects of natural nanozymes. We focus on the key scientific issues surrounding nanozymes, including how nanozymes catalyze biochemical reactions, what unique features differentiate their biocatalytic properties from those of enzymes, and how they can be objectively evaluated and compared. We also explore current research trends in nanozymes and their transformative and long-term impact on biocatalysis and other related fields such as the origin of life, evolution, pathogenic mechanisms, and so on.

Fundamental insights into nanozymes

"Nanozyme" is a compound term derived from "nanomaterial" and "enzyme," akin to the naming conventions of ribozyme, DNAzyme, and abzyme. The term "nanozyme" was introduced by Lucia Pasquato and Paolo Scrimin in 2004 to describe gold nanoparticles functionalized with triazacyclonane that catalyze transphosphorylation[45]. Subsequently, other studies adopted the term "nanozyme" for their catalysts, including a supramolecular containing four Ga^{3+} ions catalyzing acetals and ketals hydrolysis[46], and a cationic block copolymer encapsulating catalase[47]. These "nanozymes" represent nano-immobilized catalysts or enzymes, where nanomaterials act as carriers for catalytic groups.

In 2007, it was reported that Fe_3O_4 nanoparticles possess intrinsic peroxidase-like activity[28], shifting the focus of research to the inherent biocatalytic properties of nanomaterials. Inspired by this discovery and the following studies, Hui Wei and Erkang Wang published a review in 2013 that began using "nanozymes" to specifically describe "*nanomaterials with enzyme-like characteristics*"[29]. This definition has been widely adopted in the literature, prompting the discovery of new nanozymes by comparing their catalytic activity with that of enzymes. However, the term "enzyme-like" has sparked debates regarding how closely nanomaterials must resemble enzymes to be classified as nanozymes. Some viewpoints hold that nanozymes should "*exhibit some structural and/or functional resemblance to the enzyme*"[48] or should "*mimic most of the properties of enzymes, including an efficient catalytic activity and a specific mechanism for a given reaction*"[49]. Yanchao Lyu and Paolo Scrimin proposed that nanozymes must meet "*the two critical and minimal requirements: the binding of the substrate before its transformation and the knowledge of the functional groups present in the putative catalytic site*"[50]. These discussions are based on the understanding that nanozymes should or must be a type of "enzyme mimic".

An updated definition in 2021 emphasized the potential difference in catalytic mechanism between nanozymes and enzymes, and defined nanozymes as "*nanomaterials that catalyze the conversion of enzyme substrates to products and follow enzymatic kinetics*(e.g., *Michaelis–Menten*) *under physiologically relevant conditions, even though the molecular mechanisms of the reactions could be different between nanozymes and the corresponding enzymes*"[51]. More recently,

BOX 2

The material and catalytic type of nanozymes

Material type. Research on nanozymes initially focused on inorganic nanomaterials, including metal oxides like Fe_3O_4, CeO_2, and V_2O_5, metals such as Au, Ag, Pt, and Pd, and carbon nanomaterials like graphene, carbon nanotubes, and carbon dots[29,235]. Later, organic-inorganic hybrid materials such as MOFs[236], peptide-metal composites[159], metal-anchored protein assemblies[219], and organic materials like histidine-rich peptides[237] and amyloid-like peptide assemblies[43] were also reported to exhibit enzyme-like activity. These materials typically range in nanoscale and have periodically arranged nanostructures. While most nanozymes are artificially engineered nanomaterials, some natural biogenic nanozymes with biocatalytic functions have been discovered in recent years, such as the iron core in ferritin with superoxide dismutase (SOD)-like activity[42] and magnetosomes with peroxidase-like activity[41]. Therefore, nanozymes are no longer limited to inorganic and artificial substances but encompass any nanomaterial whose biocatalytic activity stems from nanoscale properties. Biological macromolecules like natural proteins and nucleic acids can also be considered nanomaterials in terms of their nanoscale size, but their catalytic activity is determined by amino acid or nucleotide sequences encoded by genes, rather than by their nanoscale properties. This distinction separates them from nanozymes.

Catalytic type. Researchers have pursued a research paradigm using established enzymatic methods to discover nanozymes since 2007[28], resulting in most nanozymes exhibiting "enzyme-like" activities and being classified similarly to enzymes. Among these, the majority demonstrate oxidoreductase-like activities, with a particular focus on peroxidase-like, oxidase-like, catalase-like, and SOD-like activities. Peroxidase-like nanozymes such as Fe_3O_4[28], Ir[139], and Os[238] primarily catalyze the oxidation of common HRP substrates such as 3,3′,5,5′-tetramethylbenzidine (TMB), 2,2′-azinobis-(3-ethylbenzthiazoline-6-sulfonate)(ABTS), and o-phenylenediamine (OPD) in the presence of H_2O_2. There are also glutathione peroxidase-like nanozymes, like V_2O_5 that use glutathione as an electron donor[121]; myeloperoxidase-like nanozymes, such as AuPd alloy that catalyze H_2O_2 with halide ions to produce hypohalous acid[239]; and lipoperoxidase-like nanozymes like CeO_2 that catalyze lipid peroxide generation[240]. Oxidase-like nanozymes, like Co_3O_4, use oxygen as the hydrogen acceptor to oxidize substrates such as TMB[241]. Other oxidase-like nanozymes catalyze specific substrates, for instance, Au nanozymes catalyzing glucose similar to glucose oxidase[240], and CuAg alloys[242] and Cu_2O[243] catalyzing like cytochrome c oxidase. Catalase-like nanozymes decompose H_2O_2 into H_2O and O_2, discernible by increased oxygen levels or bubble formation during the reaction. Studied catalase-like examples include Pt[147] and Fe–N_4 single-atom nanozymes[76]. SOD-like nanozymes, such as carbon dots[112] and Cu-MOF[244], dismutate superoxide anions ($O_2^{\bullet-}$) into O_2 and H_2O_2.

As research advances, nanozymes with biocatalytic activities beyond oxidoreductase-like have emerged, including hydrolase-like, isomerase-like, and lyase-like activities. For example, CdTe quantum dots (4.5 nm) can recognize GAT^ATC DNA sequences and induce light-triggered T^A phosphodiester bond cleavage[245]. Magnetic $CuFe_2O_4$ possesses intrinsic protease-like activity that is capable of hydrolyzing bovine serum albumin and casein under physiological conditions[246]. ZIF-8 nanoparticles with carbonic anhydrase-like activity catalytically accelerate CO_2 hydration[33]. Chiral carbon dots derived from cysteine exhibit an activity similar to topoisomerase I, enantioselectively mediating the topological rearrangement of supercoiled DNA[34]. Besides nanozymes with natural enzyme counterparts, some nanomaterials catalyze biochemical reactions that natural enzymes cannot catalyze. For example, in biological systems, MOF-Cu catalyzes azide–alkyne cycloaddition[247], and Pd nanoparticles catalyze the hydrogenation of •OH[248]. These nanomaterials should also be considered nanozymes. Collectively, these discoveries underscore the broad biocatalytic potential of nanozymes.

Mohamad Zandieh and Juewen Liu discussed the evolution of nanozymes, and suggested using "enzyme-like" to describe "*nanozymes based on the same substrate and product (as enzymes)*," and "enzyme-mimicking" to describe "*nanozymes with efforts made in mimicking the structure and function aspects of enzymes*"[52].

Nanozymes are primarily identified by their functional similarities to enzymes, particularly their ability to catalyze biochemical reactions involving the same substrates and products. However, evidence increasingly indicates that nanozymes differ fundamentally from their enzymatic counterparts in chemical structure, catalytic mechanisms, and even functions (e.g., Fe_3O_4 nanozymes versus HRP[53–56]). Therefore, it is reasonable to regard nanozymes as a distinct class of functional entities that exhibit biocatalytic characteristics rather than simple enzyme mimetics (Box 1). While nanozymes share some functional features with enzymes, they possess unique attributes that set them apart from traditional biocatalysts. They are nanoscale catalytic materials, typically ranging from a few nanometers to a few hundred nanometers in size, comparable to or larger than enzymes (e.g., catalase, ~10 nm[57]). Their biocatalytic activity results from nanoscale effects, where reduced dimensions lead to increased surface area, abundant active sites, and nano-confined spaces with unique electronic properties that facilitate substrate binding and turnover. Notably, the catalytic turnover of nanozymes is inherently driven by their nanostructure rather than by externally introduced catalytic groups, non-structural modifications, or the release of metal ions. For example, MnO_2 acts as a catalase-like nanozyme under neutral conditions, catalyzing the decomposition of H_2O_2 to produce O_2. However, under mildly acidic conditions, MnO_2 no longer behaves as a typical nanozyme because it reacts with H_2O_2 and H^+ to produce O_2 and Mn^{2+} without complete catalytic turnover[58].

Current evidence suggests that nanozyme-catalyzed reactions occur at specific surface interfaces (active sites) rather than across the entire nanoparticle or surface. Due to their structural heterogeneity, nanozymes typically possess a variety of active sites. Active sites located on particular crystal planes, with unsaturated coordination, at heterostructure interfaces, or at defects (e.g., steps, edges, corners) often exhibit higher activity[31]. This is largely attributed to the influence of local geometric structures on electron density, which promotes reactant adsorption and activation. The abundance and diversity of active sites in nanozymes enable them to catalyze multiple substrates or reaction pathways simultaneously, with potential collaborative or competitive interactions that influence overall activity. These characteristics make nanozymes versatile multivalent catalysts, although they may lead to more complex and less predictable behavior in dynamic environments. Many enzymes are highly specific, typically catalyzing only a single reaction[59]. For instance, carbonic anhydrase specifically catalyzes the conversion of carbon dioxide and water into carbonate and protons, increasing the reaction rate by 10^8 times compared to the uncatalyzed process[60]. In contrast, nanozymes are rarely characterized by strict catalytic specificity. Many nanozymes are capable of catalyzing multiple substrates, such as peroxidase-like nanozymes that oxidize various organic substrates in the presence of H_2O_2, while also facilitating the transformation of substrates through different reaction pathways,

https://doi.org/10.1038/s41467-025-62063-8

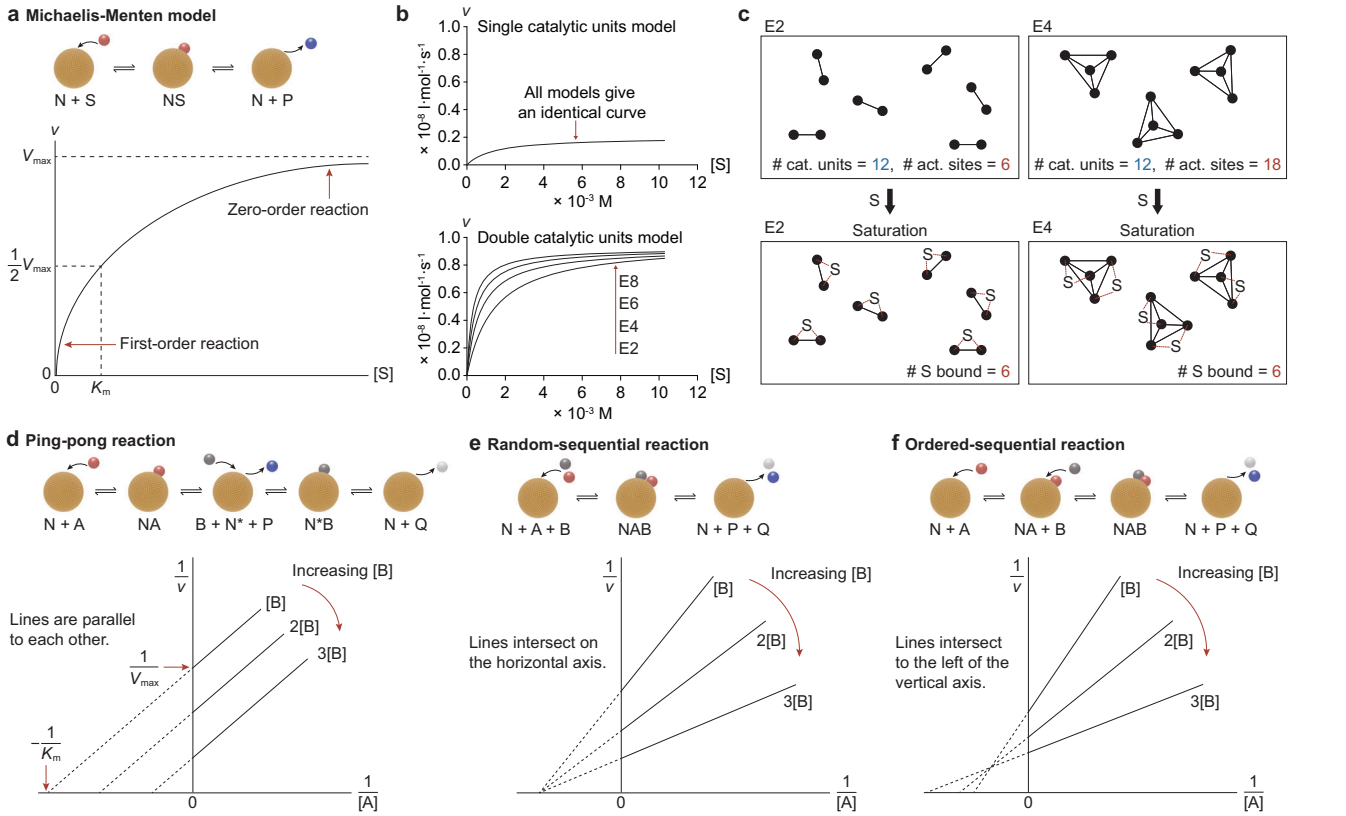

Fig. 2 | Reaction kinetic models of nanozymes. a The Michaelis–Menten kinetic model of a single-substrate reaction. Top: Schematic diagram of the reaction process. Bottom: Saturation curve showing the relation between the substrate concentration and reaction rate. **b** Calculation of the saturation behavior of the multivalent catalyst models E2–E8 for the case where the catalysis is performed by only a single catalytic unit (top) or by two catalytic units (bottom). Figure adapted from Zaupa et al.[80] **c** Effect of catalytic unit clustering on the generation of active sites in multivalent models E2 and E4. Each catalytic unit is represented by a black dot (●), and each active site is represented by a line connecting two catalytic units (−). Figure adapted from Zaupa et al.[80] Kinetic models for two substrate reactions: **d** ping-pong reaction, **e** random-sequential reaction, **f** ordered-sequential reaction.

such as decomposing H_2O_2 to produce •OH (peroxidase-like activity) or O_2 (catalase-like activity)[35].

These multi-substrate and multi-activity characteristics of nanozymes arise from several factors. First, many nanozymes exhibit oxidoreductase-like activities due to their exceptional electron transfer capacity[61,62], yet redox reactions are inherently challenging to control. These reactions involve oxygen-containing small molecules that extensively interact with biomolecules and diffuse throughout the reaction system. Many natural oxidoreductases show relatively low specificity. For example, HRP catalyzes the oxidation of various organic substrates and also exhibits catalase-like activity under neutral conditions (pH 6.5–8.5)[63]. Similarly, the most abundant cytochrome P450 enzyme CYP3A4 is responsible for metabolizing over 50% of drugs used in clinical[64]. Second, unmodified nanozymes typically possess active sites exposed on their surfaces, enabling access to various substrate molecules but often lacking specific recognition domains. Enhancing substrate selectivity in these systems can be achieved by functionalizing surfaces with molecularly imprinted polymers[65] or chiral molecules[66]. The size exclusion effect of porous structures, such as those in covalent organic frameworks (COFs) or metal-organic frameworks (MOFs), can also regulate substrate accessibility to active sites, thereby improving selectivity[67]. Third, the diversity of active sites in nanozymes, along with differences in their electronic structure, leads to variations in catalytic performance. For example, the unique d orbitals in transition metal-N interactions cause Fe-N-C and Co-N-C nanozymes to exhibit up to 200 times opposing selectivity when catalyzing the reaction of 3,3′,5,5′-tetramethylbenzidine (TMB) and luminol with H_2O_2[68].

Metrics for performance evaluation and comparison

Analyzing the catalytic kinetics of nanozymes is essential for understanding their biocatalytic functionality, particularly how they interact with substrates and their turnover rates. To ensure clarity, the "active site" here is defined as the smallest functional unit capable of independently binding substrates and catalyzing reactions, while the "catalytic unit" is a conceptual unit for analysis, which could represent a single nanoparticle, a single metal atom, or a structural component that constitutes an active site, depending on the experimental context.

Michaelis–Menten kinetics

Nanozymes frequently exhibit enzyme-like Michaelis–Menten kinetics, which is regarded as a key feature of their biocatalytic behavior. Similar to enzymes, the catalytic process at a single active site (N) of nanozyme is hypothesized to involve substrate (S) binding, intermediate complex (NS) formation, and product (P) desorption ($N + S \leftrightarrow NS \rightarrow N + P$)[69,70]. Assuming the NS complex reaches a rapid equilibrium with a constant concentration [NS], the catalytic kinetics can be described by the Michaelis–Menten Eq. (1) (Fig. 2a)[71].

$$v = \frac{V_{max} \cdot [S]}{K_M + [S]} \quad (1)$$

In this equation, v is the reaction velocity, V_{max} is the maximum reaction rate when active sites are saturated, [S] is the substrate concentration, and K_M is the Michaelis constant, which corresponds to the

substrate concentration at half of V_{max} (Fig. 2a)[71,72]. Accurate measurement of Michaelis–Menten kinetics requires specific conditions[71]: 1) The reaction involves a single-substrate (or for multiple substrates, only one concentration varies while others remain constant). 2) The step NS → N + P is irreversible, or only the initial rates are measured. 3) The initial substrate concentration [S] is significantly higher than the active site concentration [N], and [N] remains constant. 4) Other conditions that may affect the reaction rate, such as temperature, pH, and ionic strength, remain stable. For nanozymes, additional factors such as multi-activity, chemical stability, and colloidal stability must be considered. Ignoring these can lead to errors, such as underestimating the oxidase-like activity of Mn_2O_3 due to multi-activity or misattributing Au@Ag activity to intrinsic catalytic properties rather than Ag^+ ion leakage[73].

The Michaelis–Menten model is tailored for enzymes with a single active site interacting with a single-substrate[74]. Nanozymes, however, typically possess multiple active sites and interact with multiple substrates. Ideally, the kinetic analysis should, whenever feasible, be based on the concentration of active sites rather than the entire nanozyme. The number of active sites exposed on the surface of some nanozymes can be estimated by methods such as chemical adsorption, spectroscopy, and geometric estimation[75]. These methods implicitly assume that all exposed active sites on the surface are either identical or predominantly of one type. However, the surfaces of nanozymes are often heterogeneous with diverse potential active phases and sites exhibiting different substrate affinities and catalytic rates[76]. As a result, the total reaction rate represents the cumulative contributions from all active sites, as described by Eq. (2)[77,78]. Here, n represents the number of active sites, each characterized by its specific K_M and V_{max}.

$$v = \sum_{i=1}^{n} \frac{V_{max,i} \cdot [S]}{K_{M,i} + [S]} \tag{2}$$

Selective identification of these distinct active sites remains exceedingly difficult at present. In practice, the Michaelis–Menten parameters of nanozymes are usually measured as the macroscopic average of all microscopic substrate binding and catalytic events within the multivalent system, which needs to be reinterpreted to better reflect the catalytic mechanism of nanozymes.

Michaelis constant K_M. The K_M indicates the affinity between the active site and the substrate, determining the formation of NS complexes. A lower K_M generally suggests higher substrate binding affinity, although it is not equivalent to the substrate dissociation constant. The K_M is typically governed by the intrinsic properties of active sites and is independent of their concentration[79]. However, for multivalent catalysts, the apparent overall K_M may be affected by cooperative interactions between catalytic units. Giovanni Zaupa et al. developed a theoretical model to investigate how the valence of multivalent catalysts (E2–E8, with 2–8 catalytic units) impacts Michaelis–Menten parameters[80]. Their findings show that when a single catalytic unit drives the reaction, all multivalent catalysts (E2–E8) display saturation curves identical to a monomeric catalyst (Fig. 2b). However, when two catalytic units are required to form a functional active site, increasing catalyst valency raises the apparent number of active sites, thereby lowering the apparent K_M without altering the intrinsic substrate affinity of individual active sites (Fig. 2b). For example, with 12 catalytic units, a divalent system (E2) forms 6 active sites, while a tetravalent system (E4) yields 18 active sites, demonstrating an exponential increase in potential binding sites for the first substrate with higher valency (Fig. 2c). This multivalency effect influences only K_M but not k_{cat}, as the number of substrates accommodated at saturation remains constant regardless of catalytic unit arrangement[80]. This principle has been shown to apply to multivalent catalysts such as dendrimer catalysts[80] and catalytic self-assembled monolayers on Au nanoparticles[81], though its relevance to other nanozymes remains uninvestigated.

Catalytic constant k_{cat}. The k_{cat}, calculated by Eq. (3), represents the turnover rate of the complex NS converting to release N and P when the active sites are saturated with substrate[72]. Unlike V_{max}, k_{cat} is independent of the concentration of active sites, making it suitable for comparisons across different experimental systems[82].

$$k_{cat} = \frac{V_{max}}{[N]} \tag{3}$$

Accurately determining k_{cat} requires precise identification and quantification of active sites, which remains a challenge for many nanozymes. Different assumed catalytic units have been used in the literature to calculate k_{cat}, including assigning each particle, each metal atom, or each surface metal atom as the monomeric catalytic unit. An analysis conducted by Mohamad Zandieh and Juewen Liu, using Fe_3O_4 nanozymes as a case study, revealed that k_{cat} values can vary by an astonishing eight orders of magnitude when calculated based on different assumed catalytic units[83]. Assigning an entire particle as a catalytic unit overestimates k_{cat} because each particle typically contains many active sites. For nanozymes with discrete homogeneous metal sites where all metal sites are theoretically accessible to substrates, such as nitrogen-doped carbon nanozymes coordinated by single-atom metals, using the total metal content as the number of active sites can be reasonable[84,85]. However, it is essential to confirm that the single-atom metal serves as the actual active site, rather than other structures like nitrogen functionalities or carbon defects[86]. Similarly, for active sites composed of bimetallic elements, such as Fe–Fe[87], Fe–Cu[88], and Fe–Co[89], the correspondence between the metal content and the number of active sites needs to be carefully considered. For solid nanozymes, treating all metals as catalytic units underestimates k_{cat}, as only surface-exposed metals directly serve as active sites. Moreover, not all exposed surface metals are likely to function as active sites, and steric hindrance between substrates at saturation may further limit some active sites from contributing to catalysis. Thus, normalizing by total surface metals may also underestimate k_{cat}, but it should offer a lower-bound estimate. For non-metal nanozymes (such as carbon-based nanozymes), identifying active sites is even more complex, requiring an in-depth understanding of the role of heteroatoms, defects, and functional groups in catalysis. Structural factors such as lattice and pore size distribution must also be considered. When direct measurement of active sites is impractical, reaction rates can be normalized by the surface area of the nanozyme or the active phase, expressing k_{cat} in units of $s^{-1}m^{-2}$.

Specificity constant k_{cat}/K_M. The k_{cat} reflects nanozyme properties when active sites are saturated with substrate and loses its function at low substrate concentrations[90]. In industrial applications, inorganic catalysts are typically used under conditions of high substrate concentrations, and catalytic ability is usually expressed by the turnover frequency (TOF), which is equivalent to k_{cat} in enzymology[91]. In contrast, nanozymes typically function within physiologically related conditions where the substrate concentrations are low in many cases. Under these conditions, the reaction rate depends on both the substrate binding affinity (related to K_M) and the conversion rate after binding (related to k_{cat}), making both k_{cat} and K_M substantial parameters[92]. When $[S] \ll K_M$, the kinetic equation simplifies to Eq. (4). Under these conditions, the reaction rate (v) is contingent upon the concentrations of active sites [N] and substrate [S], following second-order reaction kinetics. The specificity constant k_{cat}/K_M is a measure of catalytic efficacy, useful for distinguishing between two competing substrates for the same nanozyme and for comparing the catalytic efficiencies of nanozymes with reference uncatalyzed bimolecular

https://doi.org/10.1038/s41467-025-62063-8

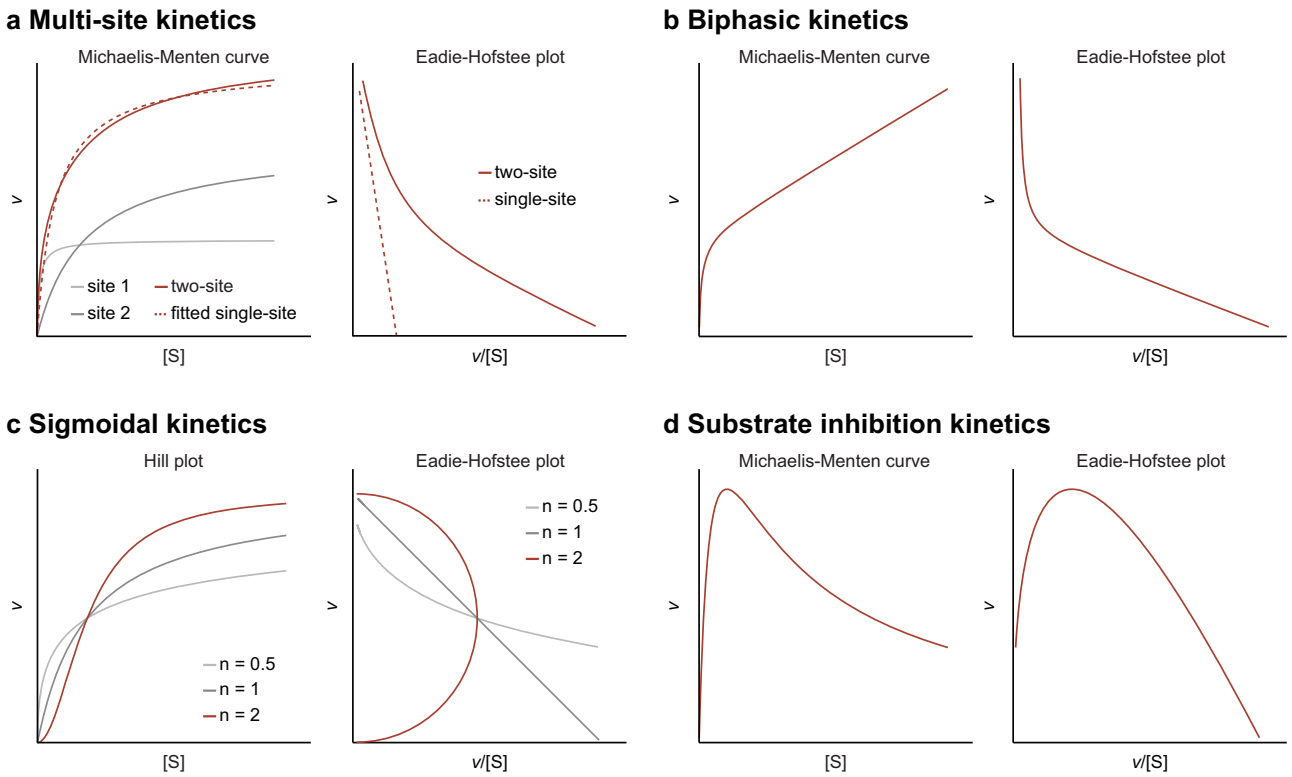

Fig. 3 | Atypical kinetics applied for nanozymes. The panels depict the υ-versus-[S] kinetic plot and the Eadie-Hofstee plot (υ-versus-υ/[S]) for **a** multi-site kinetics, **b** biphasic kinetics, **c** sigmoidal kinetics, and **d** substrate inhibition kinetics.

reactions[93]. It should be noted that k_{cat}/K_M is the rate constant for low substrate concentrations ($[S] \ll K_M$), and cannot accurately describe the catalytic efficiency when the substrate concentration is close to or higher than K_M[90,92]. Moreover, k_{cat}/K_M may not be applicable when comparing the catalytic efficiency of different nanozymes[94].

$$\upsilon = \frac{k_{cat}}{K_M} \cdot [N] \cdot [S] \tag{4}$$

Multi-substrate kinetics

Multi-substrate reactions involve more complex kinetics. For dual-substrate reactions, kinetics are often simplified by fixing the concentration of one substrate and varying the other, enabling the calculation of apparent K_M and V_{max}. There are two catalytic pathways for dual-substrate reactions: ping-pong reactions, where one product is released before all substrates bind (Fig. 2d), and sequential reactions, where both substrates must bind to the active site in a random (Fig. 2e) or specific (Fig. 2f) order before the reaction occurs[95]. For example, the peroxidase-like activity of the Fe_3O_4 nanozyme follows a ping-pong mechanism[28], while the CTAB-coated Au-CeO_2 nanozyme follows a random-sequential mechanism[96]. Experimentally, Lineweaver-Burk plots (1/υ-versus-1/[S], Eq. 5) can differentiate these mechanisms, with parallel lines suggesting a ping-pong mechanism and intersecting lines indicating a sequential mechanism[95].

$$\frac{1}{\upsilon} = \frac{K_M}{V_{max}} \cdot \frac{1}{[S]} + \frac{1}{V_{max}} \tag{5}$$

Atypical kinetics

Nanozymes with independent and uniform active sites typically follow standard Michaelis–Menten kinetics, characterized by a hyperbolic curve. However, when multiple active sites differ in their ability to bind or convert substrates, or when interactions such as allosteric effects, cooperativity, or competitive adsorption occur between active sites, the resulting υ-versus-[S] curve deviates from the standard hyperbolic function, displaying atypical kinetics. Atypical kinetics are likely widespread in nanozymes, yet detailed analyses remain scarce. Here, we apply enzymatic methods to explore these non-standard kinetic behaviors in nanozymes.

Multi-site kinetics. Nanozymes may very likely possess heterogeneous active sites with varying kinetic properties. Even if these active sites differ significantly, the overall reaction may still appear to follow a simple hyperbolic curve, masking the underlying complexity. For instance, consider a single-substrate reaction catalyzed by a nanozyme with two-type distinct active sites: one with "high affinity-low capacity" (site 1: $K_{M1} = 1$, $V_{max1} = 40$) and another with "low affinity-high capacity" (site 2: $K_{M2} = 20$, $V_{max2} = 80$). If these active sites function independently, the total reaction rate is the sum of their contributions, as given by Eq. (6).

$$\upsilon = \frac{V_{max1} \cdot [S]}{K_{M1} + [S]} + \frac{V_{max2} \cdot [S]}{K_{M2} + [S]} \tag{6}$$

The resulting kinetic curve reveals that site 2 dominates at high substrate concentrations, while site 1 prevails at lower concentrations (Fig. 3a). However, fitting the overall two-site curve to the standard Michaelis–Menten equation yields apparent single-site parameters ($K_M \approx 7.75$, $V_{max} \approx 112.09$, $R^2 = 0.98$), potentially leading to the erroneous conclusion that the reaction involves only one active site. To uncover the multi-site nature, the Eadie-Hofstee transformation (Eq. 7) is valuable[97].

$$\upsilon = -K_M \frac{\upsilon}{[S]} + V_{max} \tag{7}$$

For a single-site system, the Eadie-Hofstee plot (υ-versus-υ/[S]) is linear, while in a two-site system, it deviates from linearity, forming a

concave curve (Fig. 3a). Although rarely used in nanozyme studies, Eadie-Hofstee plots of some nanozymes exhibit concave patterns[98–100], suggesting that active-site heterogeneity may be common yet often overlooked. Therefore, we advocate incorporating Eadie-Hofstee transformation into routine kinetic analyses, especially for nanozymes composed of heterogeneous structures or composite materials, where active-site diversity likely influences catalytic performance.

Biphasic kinetics. In standard Michaelis–Menten kinetics, reaction rates plateau at high substrate concentrations. In contrast, biphasic kinetics show a two-phase curve where the rate continues to rise without saturation (Fig. 3b). For single-site systems, biphasic kinetics may arise when one active site binds two substrate molecules: the first binding saturates (low K_{M1}, low V_{max1}), while the second does not saturate (high K_{M2}, high V_{max2}) due to experimental constraints (e.g., substrate solubility), modeled by Eq. (8)[101].

$$v = \frac{V_{max1}[S] + \frac{V_{max2}}{K_{M2}}[S]^2}{K_{M1} + [S]} \tag{8}$$

In multi-site systems, biphasic kinetics can result from the combined activity of two distinct active sites: one saturates at low substrate concentrations and follows a hyperbolic curve, while the other has a very high K_M, resulting in a linear curve, described by Eq. (9)[101].

$$v = \frac{V_{max1} \cdot [S]}{K_{M1} + [S]} + \frac{V_{max2}}{K_{M2}} \cdot [S] \tag{9}$$

The Eadie-Hofstee plot of biphasic kinetics typically exhibits a concave curve (Fig. 3b)[77]. Unsaturated v-versus-[S] curves are frequently observed in nanozyme studies, but it is unclear whether this reflects insufficient substrate levels or true biphasic kinetics. Fitting such curves to the standard Michaelis–Menten equation may lead to misleading results.

Sigmoidal kinetics. When active sites interact, substrate binding at one site may influence others, leading to cooperativity and an S-shaped v-versus-[S] curve (Fig. 3c). The Hill Eq. (10) is commonly used to describe this cooperative behavior[77]. Here, S_{50} is analogous to K_M, but it also includes interaction factors[102]. The Hill coefficient n indicates the degree of cooperativity: $n > 1$ suggests positive cooperativity, while $n < 1$ indicates negative cooperativity. A larger n value corresponds to greater cooperativity and a more pronounced S-shaped curve. The cooperativity-induced curve deviation is more apparent in the Eadie-Hofstee plot, where it forms a characteristic hook shape (Fig. 3c)[77].

$$v = \frac{V_{max} \cdot [S]^n}{S_{50}^n + [S]^n} \tag{10}$$

Sigmoidal kinetics has been revealed in some nanozymes. For example, the MoO_3-TPP nanozyme, with sulfide oxidase-like activity, catalyzes sulfite oxidation in the presence of ferrocyanide, showing sigmoidal kinetics when concentrations of both MoO_3-TPP and ferrocyanide are constant[103]. The Hill coefficient $n = 2.35$ indicates positive cooperativity, likely due to competition between the sulfite anion and the negatively charged ferrocyanide on the nanoparticle surface. Sigmoidal kinetics have also been observed in the catalytic oxidation of reduced cytochrome c by MOF-808-His-Cu nanozyme[104] and the catalytic reduction of oxidized cytochrome c by PEG-HCC nanozyme in the presence of NADH[105].

Substrate inhibition kinetics. In substrate inhibition kinetics, the reaction rate initially increases with substrate concentration, reaches a peak, and then decreases as the concentration continues to rise (Fig. 3d). This is typically attributed to the simultaneous binding of multiple substrate molecules at the active site, leading to non-competitive inhibition and reduced substrate turnover[106]. The simplest model for substrate inhibition is described by Eq. (11)[77], where K_i is the inhibition constant for the second substrate molecule. However, since V_{max} is never fully reached, the accuracy of K_M obtained by this equation is compromised. The Eadie-Hofstee plot for substrate inhibition typically displays a convex curve (Fig. 3d).

$$v = \frac{V_{max}}{1 + \frac{K_M}{[S]} + \frac{[S]}{K_i}} \tag{11}$$

Some nanozymes (e.g., Au@Pt, Prussian blue) show reduced peroxidase-like activity at high substrate (TMB) levels, but this was linked to solvent-induced aggregation (e.g., DMSO effects) rather than true substrate inhibition[73].

Specific activity

For nanozymes, kinetic analysis of active sites offers insights into catalytic processes but is insufficient for evaluating the overall catalytic capacity. This capacity depends not only on the intrinsic efficiency of a single active site but also on the number of active sites and the effect of non-catalytic components. Therefore, standardized methods and units are essential to comprehensively assess the overall activity of nanozyme. Following the enzymatic standard, a nanozyme activity unit (U) is defined as the amount of nanozyme that catalyzes the conversion of 1 μmol of substrate per minute under specified conditions, including optimal pH, temperature, and substrate concentration[72,107]. The specific activity is then defined as the activity units per milligram of nanozyme (U/mg). In some applications, such as enzymatic electrodes, it might also be useful to define specific activity in units per mole of particles (U/mol), especially when the sizes of nanozymes are similar[52]. However, current limitations in accurately quantifying the number of nanoparticles may introduce errors in defining specific activity as U/mol. Some studies calculate specific activity based on units per milligram or mole of metal, but this approach does not reflect the overall activity, complicating comparisons across different batches or studies. For enzymes, specific activity is commonly used to measure the purity of enzyme preparations[108]. Similarly, for nanozymes, specific activity can be employed to compare batches of the same nanozyme or to evaluate changes in activity during preparation, storage, or recycling. In research, specific activity serves as a direct metric for comparing catalytic performance. However, this may lack objectivity when nanozymes differ in composition or density. For example, a lower-density nanozyme may exhibit higher specific activity than a denser one, without implying higher catalytic efficiency. Therefore, when comparing specific activities, factors such as composition, density, size, and surface properties should be considered in the context of the intended application. Despite these limitations, specific activity remains a valuable reference for evaluating catalytic performance, as it reflects overall capacity, which cannot be captured by active-site kinetics alone. However, it provides limited insight into specific catalytic mechanisms and cannot replace detailed kinetic analysis at the active site level.

Structure–activity relationships

Bulk structure and surficial active center

Both nanozymes and enzymes feature confined and coordinated active centers supported by bulk architectures, distinguishing them from free ions and small-molecule enzyme mimics. However, nanozymes and enzymes exhibit distinct structure–activity relationships. Enzymes consist of continuous amino acid chains that fold into a dynamic tertiary structure, undergoing conformational changes during catalysis to facilitate substrate binding and product release. The active center, composed of specific amino acids and cofactors, features a distinct geometry and microenvironment, typically buried within the protein. Substrates must pass through specific entrances to

reach the active center. This structural arrangement protects the active center, enhances substrate specificity, optimizes the catalytic microenvironment, and allows for dynamic regulation. However, mutations or damage at critical positions may disrupt the structure of the active center, severely impacting catalytic activity. In contrast, many nanozymes consist of highly crystalline or partially amorphous structures made from inorganic or organic-inorganic hybrid materials, often in a periodic arrangement[31]. These structures are generally rigid, with limited conformational changes, though some dynamic features can be introduced through surface modifications. Nanozymes made of organic materials or featuring substantial organic components in their outer shells may exhibit enhanced structural flexibility, allowing for dynamic behaviors[109]. The active centers of nanozymes are often located on the surface and exposed, comprising specific atoms and structures (such as defects or crystal faces)[31]. This arrangement improves substrate accessibility and reaction rates, enabling nanozymes to remain active even in extreme environments and achieve multifunctionality through surface modifications. Moreover, the active sites of nanozymes are relatively independent, so local structural changes have minimal impact on overall catalytic activity, conferring stability and tolerance to harsh conditions.

Simple models of active sites and active phases can be simulated through theoretical calculations combined with experimental verification. The active center structures of different nanozyme materials exhibit distinct characteristics. Metal nanozymes, such as Au, Ag, Pt, Pd, and their alloys, consist of metal atoms arranged in a tightly packed lattice, with active centers generally located on high-energy facets[110]. Metal oxide nanozymes, such as Fe_3O_4 and CeO_2, are composed of transition metal atoms and oxygen atoms arranged in a sequence. Their active centers are often surface-exposed metal atoms located at lattice defects and oxygen vacancies, which switch between oxidation states to mediate electron transfer[111]. In carbon-based nanozymes, such as carbon nanotubes and carbon dots, active centers are found at structural defects, edge carbon atoms, or functionalized modification sites. The conjugated π-electron system of carbon materials enables electron transfer with substrates, while functional groups (such as hydroxyl, carboxyl, carbonyl, etc.) help adsorb substrates and accelerate electron transfer[112]. MOF nanozymes are composed of metal ions (such as Zn^{2+}, Cu^{2+}, etc.) coordinated with organic ligands (such as imidazole, carboxylic acid, etc.), where the metal center cooperates with ligand functional groups to perform catalysis[113]. Additionally, single-atom nanozymes ($M–N_x–C$, M=Fe, Mn, Cu, Zn, etc.) feature dispersed metal atoms on carbon-based materials coordinating with nitrogen atoms to form active centers with a coordination environment similar to that of metal porphyrins[85].

Compared to active center structures simulated from single-crystal material models, real active centers are more complex influenced by defects, surface coordination, and adsorption environments, and polycrystalline or amorphous states. Identifying and simulating these real active center structures remains challenging due to the limitations of detection methods and computational power. Determining the active centers of composite materials is even more difficult, as it involves additional factors such as heteroatoms, heterostructures, interface structures, and active site synergy.

Catalytic pathway

Even when catalyzing the same substrate and producing the same product, nanozymes may follow different catalytic pathways compared to enzymes. As for oxidoreductase-like nanozymes, the catalytic pathways of nanozymes may include mediating electron transfer between substrates, and producing free or bound reactive species, and these pathways may exist simultaneously on one nanozyme[114]. A well-discussed example is the peroxidase-like activity of the Fe_3O_4 nanozyme.

In the double-substrate reaction, HRP first binds to H_2O_2, which then reacts with Fe^{III} in the active center iron porphyrin to generate an activated Fe^{IV}=O high oxidation state intermediate (Fig. 4a). This intermediate undergoes a two-step redox reaction with the double electron donor substrate, releasing the oxidized product and returning to the stationary Fe^{III} state[55,115,116]. Similarly, Fe_3O_4 nanozymes catalyze the oxidation of electron donor substrates in the presence of H_2O_2, in an optimal catalytic environment (acidic) similar to that of HRP, producing the same products. However, in the peroxidase-like reaction catalyzed by Fe_3O_4, H_2O_2 is catalyzed to form •OH, which then oxidizes the electron donor substrate to generate H_2O and oxidized products (Fig. 4b)[28]. Electron spin resonance has detected the presence of •OH and HO_2• (generated by the oxidation of H_2O_2 by •OH) radicals, although it remains unclear whether these radicals are free or adsorbed on the surface of the nanozyme. Unlike free ferrous ions that mediate the Fenton reaction, the iron in Fe_3O_4 nanozymes is confined within the nanostructure, forming active sites with electron transfer capabilities. Studies have shown that the iron content (21.2 μg/L) released by Fe_3O_4 nanozymes in the peroxidase-like catalytic system is about two orders of magnitude lower than the concentration (1 mg/L) required for the Fenton reaction and exhibits negligible reaction activity[28,117]. This indicates that the catalytic effect is due to the nano-confined Fe sites rather than free iron ions.

There are two types of iron (Fe^{II}/Fe^{III}) with tetrahedral or octahedral coordination in the crystal nanostructure of Fe_3O_4 nanozymes. Since the catalytic action primarily occurs on the surface or interface of the particles, it is widely believed that only the Fe^{II} on the surface of Fe_3O_4 nanozymes dominates the reaction process of catalyzing H_2O_2 to produce •OH[118]. This Fe^{II} is regenerated by the reaction of surface Fe^{III} with HO_2•, thereby enabling catalytic turnover and continuous reaction progress. However, recent research indicates that the active Fe^{II} on the surface of Fe_3O_4 nanozymes is difficult to recover after being oxidized by H_2O_2[53]. Instead, the internal Fe^{II} transfers its electrons to the surface layer through the $Fe^{II}–O–Fe^{III}$ chain in the structure (Fig. 4c). This process, combined with the outward migration of excess oxidized Fe^{III}, regenerates the surface Fe^{II} and sustains the catalytic reaction. Over time, as the catalytic action continues, Fe_3O_4 is slowly oxidized to γ-Fe_2O_3, leading to the depletion of its enzyme-like activity.

There is evidence that the Fe_3O_4 nanozyme surface not only forms •OH radicals but also catalyzes peroxidase-like reactions through the formation of high-valent Fe^{IV}=O species, with competition between the two pathways[54]. This finding illustrates that the Fe_3O_4 nanozyme combines characteristics of both Fenton-like catalysis (•OH radical pathway) and HRP-like catalysis (Fe^{IV}=O intermediate pathway). Recent studies indicate that the peroxidase-like activity of Prussian blue nanozymes also involves both pathways, with low-crystallinity Prussian blue forming Fe^{IV}=O intermediates more significantly than high-crystallinity counterparts[119]. However, the molecular mechanisms and structure–activity relationships determining the direction of these two pathways are not fully understood.

As a semiconductor, Prussian blue nanozyme has two possible electron transfer pathways in catalyzing peroxidase-like reactions (Fig. 4d)[119]. One is the valence band-mediated pathway, where Prussian blue first donates electrons to H_2O_2 and then obtains electrons from the reducing substrate. The other is the conduction band-mediated pathway, where the Prussian blue nanozyme or its pre-oxidized state first obtains electrons from the reducing substrate and then transfers the electrons to H_2O_2. The key to determining the electron transfer pathway is whether the valence band and conduction band energy levels of the Prussian blue nanozyme lie between the energy levels of H_2O_2 and the electron donor substrate (Fig. 4e). Unlike the depletable peroxidase-like activity of the Fe_3O_4 nanozyme, the peroxidase-like and catalase-like activities of the Prussian blue nanozyme increase with each successive round of catalysis[119]. This is because the irreversible oxidation of Prussian blue by H_2O_2 leads to an increase in the valence

https://doi.org/10.1038/s41467-025-62063-8

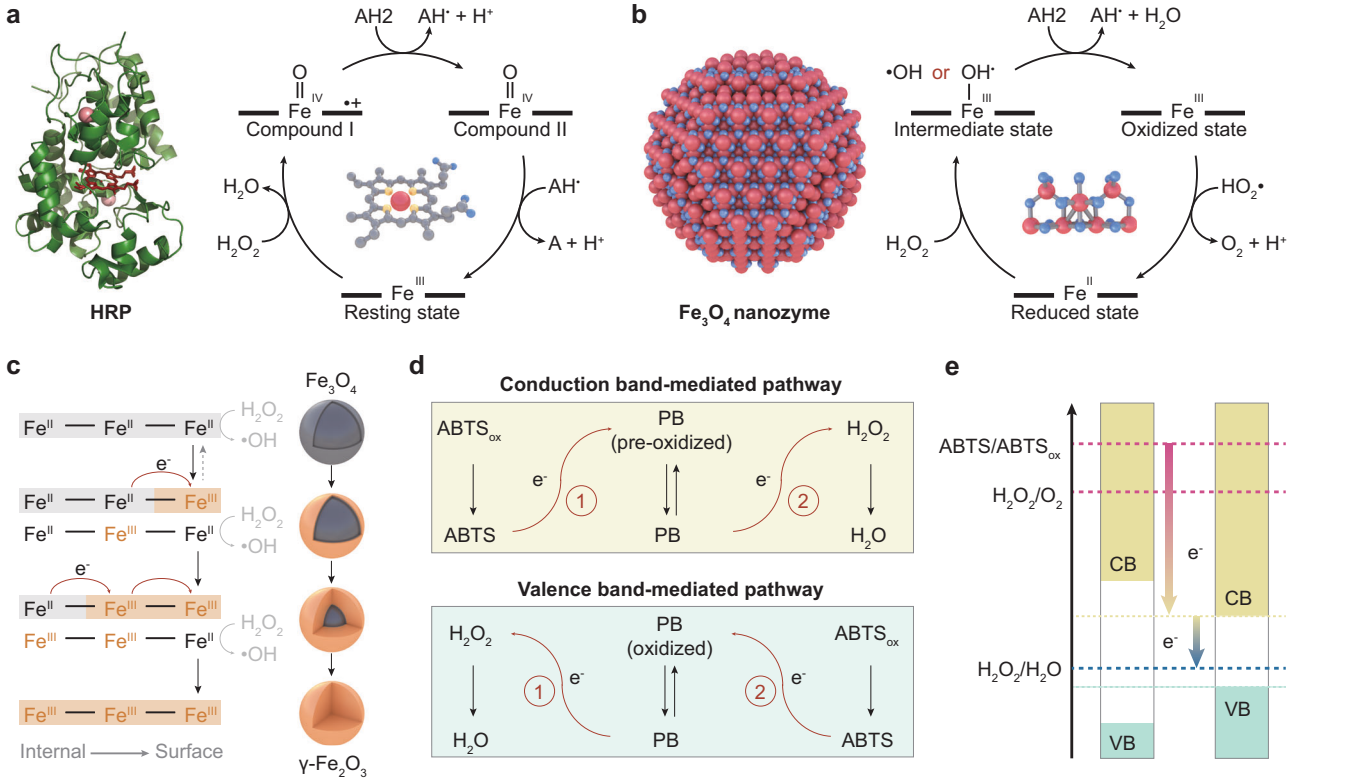

Fig. 4 | Catalytic pathways and mechanisms of nanozymes. a HRP mediates the peroxidation of the reducing substrate (AH_2) by catalyzing H_2O_2 to generate Fe^{IV}=O intermediates in the active center of iron porphyrin. **b** Fe_3O_4 nanozymes mediate the peroxidase-like reaction by catalyzing H_2O_2 to generate free or adsorbed •OH through surface-confined Fe^{II}, which differs from HRP. **c** Fe_3O_4 nanozymes regenerate surface Fe^{II} for peroxidase-like catalysis by transferring electrons from internal Fe^{II} to the surface, during which Fe_3O_4 gradually depletes its activity and transforms into γ-Fe_2O_3. Figure adapted from Dong et al.[53]. **d** Prussian blue (PB) nanozymes may have two electron transfer pathways in the peroxidase-like catalysis process: the conduction band (CB)-mediated pathway, where PB first obtains electrons from the reducing substrate, or the valence band (VB)-mediated pathway, where PB first donates electrons to H_2O_2. Figure adapted from Feng et al.[119]. **e** The dominant electron pathway is determined by whether the energy level of the CB or VB is between the energy levels of H_2O_2 and the reducing substrate. Figure adapted from Feng et al.[119]. ABTS, 2,2′-azinobis-(3-ethylbenzthiazoline-6-sulfonate).

state of surface Fe and the formation of Fe^{IV}=O, enhancing the conduction band or valence band-mediated electron transfer pathways and thereby promoting catalytic activity.

Key structural parameters

Changes in structural factors (e.g., size, morphology, doping, coordination form, surface modification) that affect the surface properties can alter the number or structure of the active sites on nanozymes, thereby affecting the catalytic activity and catalytic pathway[31].

Size and morphology. The surface area exposed by a nanozyme directly affects the number of active sites. Smaller nanozymes typically exhibit larger specific surface areas, which results in more exposed active sites and enhanced catalytic activity. For example, the peroxidase-like activity of Fe_3O_4 nanozymes decreases with increasing particle diameter (30 > 150 > 300 nm)[28]. Changing the pore size and morphology also affects catalytic activity by changing specific surface area. Flower-shaped Mn_3O_4 nanozymes, for instance, demonstrate higher superoxide dismutase (SOD)-like, GPx-like, and catalase-like activities compared to other morphologies (cube, polyhedron, hexagonal plate, and flake), attributed to their increased specific surface area[120]. In addition, different morphologies expose distinct crystal facets and active phases. For example, V_2O_5 nanozymes with exposed (010) facets exhibit higher GPx-like activity than those with other facets[121]. The regulation of crystal facets may also influence substrate activation pathways and catalytic types. For example, cubic CeO_2 nanozymes with exposed (100) facets exhibit specific peroxidase-like activity but lack haloperoxidase-like activity, while octahedral CeO_2 nanozymes with exposed (111) facets show the opposite trend[122].

Heteroatoms and heterostructures. Introducing heteroatoms or creating heterostructures on the surface of nanozymes can alter charge distribution, making the existing active sites more active or introducing new active sites. For example, Praseodymium (Pr) doping in CeO_2 nanozymes results in the formation of a lower energy band that more effectively accepts electrons from the substrate TMB, thereby increasing oxidase-like activity[123]. Similarly, introducing nickel (Ni) on the surface of $CoMoO_4$ forms Ni–O–Co bonds at the heterostructure interface, accelerating electron transfer and enhancing both oxidase-like and peroxidase-like activities[124]. In addition, sites at defect edges may be more active. Compared to single-atom nanozymes with an intact Fe–N_4–C configuration, those with defective Fe–N_4–C active sites at pore edges possess more net charge and asymmetric electrons, leading to higher catalase-like activity[76].

Coordination environment. The coordination environment of the active center stabilizes metal sites and regulates electron density, profoundly affecting activity and selectivity. In M–N_x–C single-atom nanozymes, the coordination number of the first coordination shell influences the electronic state of the metal site[125]. For example, Fe–N_5–C, constructed by adding an N coordination on the axial direction of the Fe–N_4–C coordination plane, more efficiently adsorbs O_2 and activates O–O bonds, resulting in higher oxidase-like activity[85]. Replacing N in the first coordination shell with heteroatoms may also modulate catalytic activity. For example, Fe–N_3P–C, formed by

substituting one N atom around the Fe–N_4–C center with a P atom, exhibits enhanced peroxidase-like activity by reducing the energy barrier for surface O and OH species[84]. The second coordination shell also impacts the activity of single-atom nanozymes. For example, sulfur functionalization in the second shell alter the electronic structure of the Fe–N_4 site, increasing the electron density at the Fermi level and enhancing electron transfer from the active site to the key intermediate HO_2•, thereby boosting oxidase-like activity[126].

Surface modification. Surface modification is commonly employed to improve the stability, dispersibility, and functionality of nanozymes[127]. While it may partially shield active sites, surface modification may also enhance catalytic efficiency by promoting the binding and conversion of substrates. For example, modifying the surface of Fe_3O_4 nanozymes with histidine increases their affinity for H_2O_2 by 10-fold and increases their k_{cat}/K_M of peroxidase-like activity by 20-fold[128]. Similarly, cysteine modification on Au nanozymes enhances peroxidase-like activity through electrostatic attraction with the substrate TMB[129]. Surface modification with fluoride (F^-) on CeO_2 nanozymes regulates chromogenic substrate adsorption via electrostatic interactions and promotes charge transfer during catalysis, resulting in a 100-fold increase in oxidase-like activity[130]. Constructing a TMB binding pocket on the Fe_3O_4 surface using molecular imprinting polymers increases peroxidase-like specificity for TMB nearly 100-fold[65]. In addition, CeO_2 nanozymes modified with chiral phenylalanine selectively bind to and oxidize chiral dopamine substrates[131].

Calculation and prediction

Identifying key structural parameters helps pinpoint the real active sites and simulate catalytic processes using first-principle theoretical calculations. Theoretical calculations help reveal crucial structure–activity relationships and establish predictive models. For example, the adsorption energy of •OH ($E_{ads,\ OH}$) has been proposed as a theoretical descriptor for predicting the peroxidase-like activity of iron oxide nanozymes[132]. An $E_{ads,\ OH} \approx -2.6$ eV indicates the strongest peroxidase-like activity, while values significantly above or below this threshold limit activity due to difficulties in forming or reducing active intermediates on the surface. Similarly, the e_g occupancy has been proposed as a descriptor for peroxidase-like activity in perovskite oxides[133]. An e_g occupancy around 1 correlates with the highest catalytic activity, whereas e_g occupancies of 0 or 2 correlate with lower activity. In addition, with the development of artificial intelligence, machine learning is becoming a means of predicting nanozyme performance and designing materials, and has been used in the development of SOD-like and peroxidase-like nanozymes[134,135].

Biocatalytic characteristics

Nanozymes differ from enzymes in both bulk structure and active site composition, leading to distinct biocatalytic properties. Indeed, the structures of different nanomaterials vary greatly, which means that each nanozyme may have its unique function. Here, we summarize some common biocatalytic characteristics of nanozymes.

High activity at multi-level

Nanozymes demonstrate high activity across multiple levels, including single-site, single-particle, and single-mass (specific activity) (Fig. 5a). Many enzymes have evolved highly efficient active sites, such as the catalase with a k_{cat}/K_M (4×10^7 M^{-1} s^{-1}) near the diffusional limitation (10^8–10^9 M^{-1} s^{-1})[136]. In contrast, the catalytic efficiency of single active sites in many nanozymes falls short of that in enzymes. However, this efficiency can be enhanced by mimicking the active centers of enzymes, including the effects of amino acid residues and cofactors within their catalytic microenvironments[125,137]. For instance, the Fe–N_5–C single-atom nanozyme, designed to mimic the iron coordination in heme, exhibits an oxidase-like activity against TMB substrate with a k_{cat} (based on total metal content) 79 times higher than commercial Pt/C catalysts and 30-1000 times higher than other oxidase-like nanozymes[85]. Similarly, the peroxidase-like activity of the Fe–N_3P single-atom nanozyme, mimicking heme iron coordination, shows a k_{cat} (based on total metal content) 60 times higher than Fe_3O_4 nanozyme against TMB and a k_{cat}/K_M 12.17 times higher than that of HRP[84].

Despite individual active sites in nanozymes being less efficient, the overall catalytic activity of a single nanozyme particle may rival or even exceed that of enzymes due to the multitude of active sites present. For example, the turnover rate of each surface iron atom in a 300-nm Fe_3O_4 nanozyme ($k_{cat} = 9.2 \times 10^{-3}$ s^{-1}) is five orders of magnitude lower than that of HRP ($k_{cat} = 4.0 \times 10^3$ s^{-1}), while the turnover rate of a single-particle ($k_{cat} = 3.02 \times 10^4$ s^{-1}) surpasses that of HRP ($k_{cat} = 4.0 \times 10^3$ s^{-1}) by 7.55 times[28,83]. In another example, the turnover rate of catalase-like activity at a single active site on the surface of a 4-nm Pt nanozyme ($k_{cat} = 3.0 \times 10^2$ s^{-1}) is about 100 times lower than that of natural catalase ($k_{cat} = 3.2 \times 10^4$ s^{-1}), while the turnover rate of a single Pt particle (similar in size to catalase) ($k_{cat} = 2.0 \times 10^5$ s^{-1}) is higher than that of catalase ($k_{cat} = 1.3 \times 10^5$ s^{-1})[138]. Activity comparison at the single-particle level provides valuable insights in specific scenarios, such as in vivo applications, where the number of particles reaching the target site is constrained. Under these conditions, nanozymes with higher single-particle catalytic efficiency are better suited to achieve meaningful outcomes. This efficiency is influenced by both the intrinsic activity of active sites and their number within a particle. To ensure accurate and meaningful single-particle comparisons, it is essential to conduct detailed kinetic analyses of the active sites to confirm their ability to bind substrates and maintain catalytic performance under the intended application conditions.

Beyond high single-particle activity, some nanozymes exhibit higher specific activities compared to enzymes. For example, the peroxidase-like activity of ruthenium (Ru) nanozymes modified with polystyrene sulfonate (PSS) reaches 2820 U/mg, which is more than twice that of HRP at 1308 U/mg[139]. PSS readily accepts negative charges from Ru, reducing the affinity between Ru and •OH, thereby enhancing catalytic activity. In another example, the SOD-like activity of carbon dot nanozymes prepared from activated charcoal reaches 10,767 U/mg, surpassing that of natural SOD at 4743.8 U/mg[112]. The high activity of carbon dot nanozymes is attributed to their rich surface functional groups, in which hydroxyl and carboxyl groups serve as binding sites for the substrate $O_2^{\bullet-}$, while the carbonyl group coupled to the π system serves as the catalytic site. In addition to the optimized active sites, the high mass ratio of active components in these nanozymes further boosts their specific activity by ensuring a large proportion of the material is involved in the catalytic process.

Multiple biocatalytic activities

Most enzymes have a specific type of active site and tend to exhibit a single-type catalytic activity. In contrast, nanozymes have numerous and diverse active sites exposed on the surface, enabling them to catalyze various reactions under the same or different conditions. For example, CeO_2 nanozymes have been reported to exhibit SOD-like[140], catalase-like[141], peroxidase-like[142], oxidase-like[143], phosphotriesterase-like[144], and phosphatase-like[145] activities (Fig. 5b). The optimal catalytic conditions for each biocatalytic activity may be different. For example, Fe_3O_4 nanozymes catalyze H_2O_2 to generate •OH (peroxidase-like) under acidic conditions and catalyze H_2O_2 to generate O_2 (catalase-like) under neutral conditions[146]. Many nanozymes, such as Pt[147], Co_3O_4[148], Prussian blue[149], etc., exhibit similar pH-switching dual-enzyme activities[150].

Nanozymes may carry out cascade reactions involving multiple catalytic activities under the same conditions, often leading to enhanced efficiency in catalysis (Fig. 5b). For example, on CeO_2 nanozymes, Ce^{3+} and Ce^{4+} sites facilitate SOD-like and catalase-like activities, respectively, with the potential for cascaded conversion of

https://doi.org/10.1038/s41467-025-62063-8

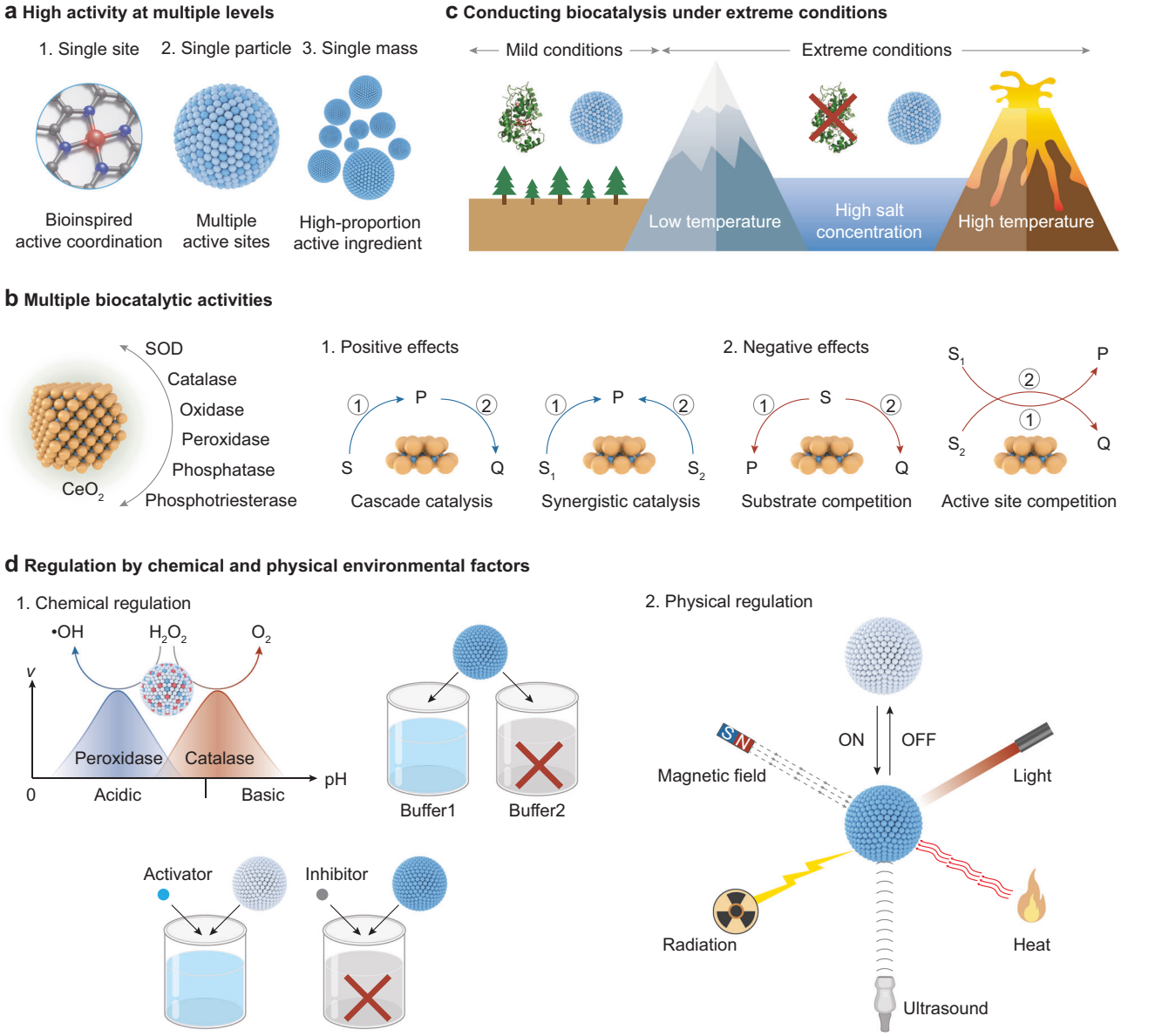

Fig. 5 | Biocatalytic characteristics of nanozymes. a Nanozymes may exhibit high activity on multiple levels: at the single-site level, particularly when they possess enzyme-like active coordination structures; at the single-particle level, owing to the presence of multiple active sites; and at the single-mass level (specific activity), due to the high proportion of active ingredients relative to the overall mass. **b** Many nanozymes possess multiple biocatalytic activities, such as CeO_2 (left), which can cascade or synergize to positively promote the reaction process. However, they may also produce negative effects due to competition for substrates or active sites. **c** Unlike most enzymes that only catalyze under mild physiological conditions, some nanozymes can catalyze biochemical reactions under extreme conditions such as low temperature, high temperature, and high salt concentration. **d** The activity of nanozymes is influenced by chemical factors such as pH, buffer composition, and some small molecules or ionic inhibitors or activators, and responds to physical stimuli such as heat, light, magnetism, radiation, and ultrasound. SOD, superoxide dismutase.

$O_2^{\bullet-}$ into O_2 and H_2O[151,152]. However, uncontrolled multi-enzyme activity may have negative effects, such as competition for substrates or active sites, which diminish desired reactions or catalyze unintended ones. For instance, Pt nanozymes concurrently exhibit peroxidase-like and catalase-like activities in specific conditions that compete for H_2O_2[138]. Therefore, comprehensive research is essential to discern whether these multiple activities stem from distinct or shared active sites and to investigate the catalytic kinetics governing these interactions. This includes understanding issues like active site competition, catalytic order, and mass transfer dynamics between multiple reactions.

The regulation of multi-enzyme activities in nanozymes often involves modifying their surface structures. For example, lithium (Li) doping in $ZnMn_2O_4$ improves SOD-like activity and activates catalase-like and GPx-like activities by converting Mn valence from +3 to +4[153]. However, balancing multi-enzyme activities in nanozymes is still challenging, as enhancing one may compromise another. To achieve effective multi-enzyme catalysis, a common strategy involves combining nanozymes with complementary dominant activities. For example, a composite nanozyme comprising carbon dots and Pt nanoparticles combines the high SOD-like activity of carbon dots with the robust catalase-like activity of Pt nanoparticles[154]. Such cascades of different nanozymes may also improve reaction selectivity, as seen in the cascade of oxidase-like N-doped carbon nanozymes and peroxidase-like Prussian blue, which enhanced the selectivity of ascorbic acid oxidation by 2000 times[155].

Conducting biocatalysis under extreme conditions

Most enzymes function optimally under mild conditions, with only a few exceptions found in extremophilic microorganisms. In contrast, many nanozymes sustain biocatalytic activity under extreme conditions such as high temperatures and high salt concentrations (Fig. 5c). Given the widespread presence of numerous inorganic nano-minerals in nature, this characteristic might explain the occurrence of biocatalysis under extreme conditions, such as those on early Earth. It also provides a foundation for developing biocatalytic applications in extreme environments, such as volcanoes, polar regions, or deep-sea habitats.

Many nanozymes exhibit thermal stability. For example, the laccase-like activity of Fe_1@CN-20 nanozyme remains nearly unaffected even after 45 min of pretreatment at 100 °C, whereas natural laccase sharply declines at 70 °C and becomes almost inactive by 80 °C[156]. Due to thermal stability, nanozymes often demonstrate robust performance at temperatures above physiological ranges. For example, the peroxidase-like activity of porous nanorod CeO_2 remains almost constant within the range of 4–60 °C, whereas the activity of HRP declines rapidly above 40 °C[142]. Interestingly, some nanozymes retain high catalytic activity at low temperatures. For example, nMnBTC nanozymes maintain stable oxidase-like activity between 0 and 45 °C and remain catalytically active to inactivate the H1N1 influenza virus even at −20 °C[157]. Another study showed that the catalase-like activity of a single Pt nanozyme was able to convert more than 1200 H_2O_2 molecules per second at 0 °C, while a natural catalase only processed 550 H_2O_2 molecules per second at the same temperature[138]. The catalytic mechanism of cold-adaptive nanozymes at low temperatures is still unclear but may be related to the numerous active sites exposed on their surfaces, which facilitate substrate interaction even at low temperatures.

High ionic strength affects the charge distribution and spatial structure of enzymes and reduces the solubility of enzymes (salting-out effect), making many enzymes intolerant to high salt concentrations. In contrast, some nanozymes exhibit tolerance to high salt concentrations and even have halophilic properties. For example, high concentrations of NaCl inactivate laccases[158], while the laccase-like activities of nanozymes such as CH-Cu (the coordination of Cu^+/Cu^{2+} with a cysteine-histidine dipeptide)[159], I-Cu (imidazole-Cu)[160], Cu/GMP (guanosine monophosphate coordinated copper)[161], and Cu_2O[162] increase with high NaCl concentrations, as NaCl promotes the adsorption of substrates on the surface of these nanozymes.

Regulation by chemical and physical environmental factors

Like enzymes, the catalytic activity of nanozymes is influenced and regulated by their surrounding environment (Fig. 5d). Because the active sites are exposed on the surface, nanozymes may be more sensitive to environmental factors. However, unlike enzymes, which undergo irreversible changes in structure and function due to harsh influences, nanozymes typically experience limited and reversible structural changes. This characteristic allows for the regeneration and recycling of nanozymes, which is important for reducing costs and enhancing sustainability. Moreover, the unique physicochemical properties of nanomaterials enable the catalytic activity of nanozymes to be regulated by various physical factors, such as heat, light, sound, and magnetism. This makes nanozymes more controllable and adaptable than enzymes in biocatalytic applications.

Chemical regulation. Unlike enzymes, which become inactive outside the working pH due to conformational changes or structural disruption, many nanozymes demonstrate structural stability over a broad pH range. For instance, citric acid-capped Pt nanozymes retain their morphology, monodispersity, and stability from pH 4.5–9.0[138], and PEI-encapsulated Prussian blue remains structurally intact within pH 3 to 11[149]. Despite the structural stability, the catalytic activity of nanozymes exhibits pH dependence, varying across different types of catalytic activities[163]. For example, the optimal pH for the peroxidase-like activity of nanozymes such as Fe_3O_4[28], Pt-Ft[147], and irregular-shaped Pt[164], and for the oxidase-like activities of nanozymes such as Cu-MOF[165], N-doped carbon dots[166], and Pd@Ir[167] typically ranges from 3 to 5. This is partially explained by that the commonly used substrates TMB forms dimeric oxidized oxTMB at pH 3 to 5 with the characteristic peak at $\lambda = 650$ nm shifting outside this pH range[138]. In contrast, nanozymes exhibiting catalase-like activity often operate optimally under neutral to alkaline pH conditions, as seen in Prussian blue[168], and Fe-N_4 single-atom nanozymes[76]. The pH dependence of nanozymes may be attributed to differences in redox reactivity and the stability of nanozymes, substrates, and products at varying pH levels as well as their interactions, such as substrate adsorption and product desorption, which jointly influence the overall pH dependence of nanozymes[150].

In addition to pH, nanozymes are also affected by other chemical factors present in the catalytic environment. For example, acetate, HEPES, and TRIS buffers have been observed to strongly inhibit the catalase-like activity of Pt nanozymes, possibly due to surface site blocking or poisoning by buffer components[138]. In contrast, phosphate buffer showed only minimal effects on Pt nanozyme activity. Similarly, the peroxidase-like activity of Ni/Co LDHs was notably slower in phosphate buffer compared to water or TRIS buffer, possibly due to surface structure alteration caused by the coordination of surface Co and Ni ions with phosphate[169].

Some chemical inhibitors and activators have been identified that modulate nanozyme catalysis. For example, phosphate inhibits the SOD-like activity of CeO_2 nanozymes by forming cerium phosphate with Ce^{3+} on the surface, which blocks the Ce^{3+}/Ce^{4+} conversion necessary for catalysis[170]. High concentrations of guanidine hydrochloride (0.4 M) reversibly inhibit the peroxidase-like activity of Fe_3O_4 by competing with H_2O_2 for iron atoms[171]. Hg^{2+} enhances the peroxidase-like activity of citrate-capped Au nanozyme by altering surface properties[172]. ATP enhances the peroxidase-like activity of Fe_3O_4 nanozymes at pH 7.4, likely by forming a stable complex with Fe_3O_4 that accelerates H_2O_2 decomposition to generate •OH[173]. Moreover, the active sites on the surface of the nanozymes may be blocked by the products. For instance, Au-catalyzed glucose oxidation exhibits rapid self-limitation because the gluconic acid products passivate the surface[174]. Studies on inhibition and activation mechanisms are essential for elucidating active sites and chemical mechanisms. More detailed kinetic analyses are needed to fully understand how these chemical factors influence the performance of nanozymes across different applications.

Physical regulation. Nanozymes composed of specific materials may alter their surface properties in response to physical stimuli such as heat, light, sound, and magnetism, thereby influencing their catalytic activity. For many thermostable nanozymes, heating typically enhances catalytic activity due to increased molecular motion and improved substrate interactions. For example, the heat-enhanced catalase-like activity has been shown in nanozymes such as Co_3O_4 (20–55 °C)[175], Pt (0–70 °C)[138], Pt-Ft (4–85 °C)[147], and Fe-SANzyme (10–70 °C)[76]. Nevertheless, the apparent catalytic activity of nanozyme may decrease at high temperatures due to the thermal decomposition of substrates or products. For example, the peroxidase-like activity of Fe_3O_4[28], Au[72], carbon[72], and FeN_3P single-atom nanozymes[84] diminishes when the temperature reaches 50–60 °C, which may be related to the thermal instability of the product oxTMB[176].

Exploiting the heat-mediated properties, photothermal nanozymes such as Au@CeO_2[177] and PtSn[178], as well as magnetothermal nanozymes such as Fe_3O_4[179] have been engineered. These materials respond to light or alternative magnetic fields to elevate their temperature, thereby enhancing catalytic performance. Radiation may

also boost the activity of nanozymes by accelerating electron transfer and valence state conversion of active sites. For example, in a composite nanozyme composed of SnS_2 nanosheets and Fe_3O_4 quantum dots, X-ray irradiation triggers the transfer of electrons from SnS_2 to Fe_3O_4, promoting the regeneration of Fe^{II} and enhancing the peroxidase-like activity for generating •OH from H_2O_2[180]. In another study, X-ray irradiation enhances the peroxidase-like activity of Fe-N_4-C single-atom nanozymes by accelerating the conversion of Fe^{III} to Fe^{II}[181]. Ultrasound has also been explored to regulate the activity of nanozymes. For instance, ultrasonic vibrations generate micropressure that induces a continuous separation and accumulation of positive and negative charges on the surface of piezoelectric tetragonal barium titanate. This effect enhances the binding of few-layer MoS_2 nanosheets, which are fabricated on its surface, to H_2O_2 and lowers the energy barrier for H_2O_2 decomposition, thus boosting the generation of •OH[182]. These stimuli-responsive characteristics enable remote control of nanozyme activity, offering advantages in applications such as medical diagnostics and treatments compared to traditional biocatalysts.

Significance of nanozymes-expanded biocatalysis

Natural role

Nature abounds with nanomaterials formed through natural physical, chemical, or biological processes, widely present in geological, biological, and environmental systems. Recently, natural nanomaterials found in organisms, such as magnetosomes and the iron core of ferritin, have been discovered to possess biocatalytic functions. Magnetosomes are magnetic Fe_3O_4 nanoparticles enveloped by a lipid bilayer membrane synthesized by magnetotactic bacteria (Fig. 6a). Studies have found that magnetosomes have peroxidase-like activity, a property shared with typical Fe_3O_4 nanozymes. However, unlike other Fe_3O_4 nanozymes that generate reactive oxygen species (ROS) during

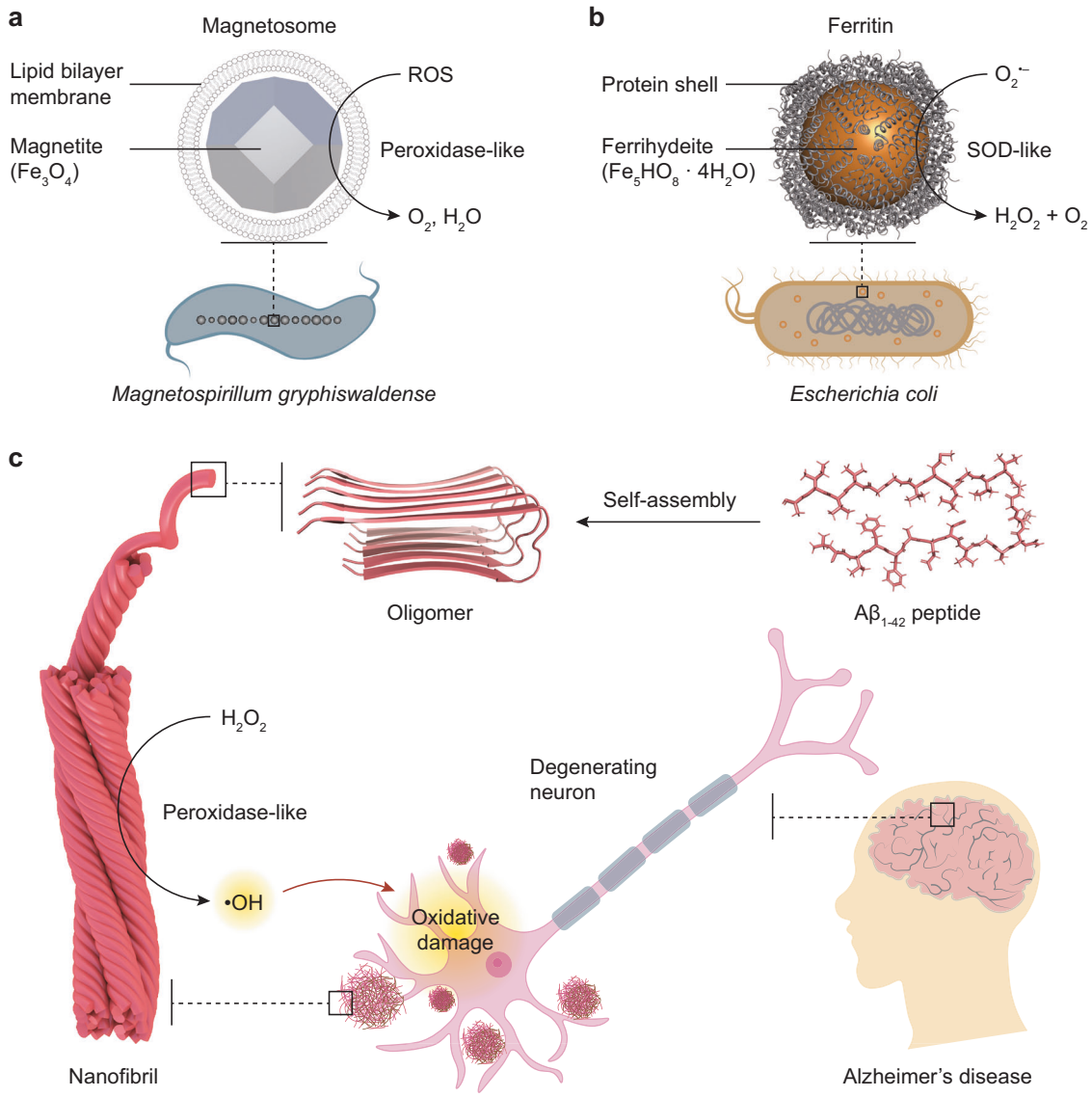

Fig. 6 | Physiological and pathological effects of natural nanozymes. **a** Magnetosomes in *Magnetospirillum gryphiswaldense* are natural nanozymes composed of Fe_3O_4 enclosed in a lipid bilayer membrane. These nanozymes exhibit peroxidase-like activity, but unlike other Fe_3O_4 nanozymes that generate reactive oxygen species (ROS), they scavenge intracellular ROS. This scavenging effect likely results from the restricted release of generated radicals, retained on the surface of the Fe_3O_4 core or confined by the lipid membrane, or from potential catalase-like activity under neutral pH conditions in the bacterial cytoplasm. **b** Recombinant ferritin expressed by *Escherichia coli* contains an iron core with ferrihydrite as the main component, functioning as a superoxide dismutase (SOD)-like nanozyme with antioxidant properties. **c** Nanoaggregates formed by the $A\beta_{1-42}$ peptide exhibit peroxidase-like activity, producing reactive oxygen species that may contribute to neuronal degeneration in Alzheimer's disease.

peroxidase-like catalysis[28], magnetosomes eliminate intracellular ROS[41]. Typically, peroxidase-like activity produces free radicals, some of which are readily released and cause oxidative damage, as seen with typical Fe_3O_4 nanozymes. In contrast, other radicals are adsorbed onto active sites, such as those in HRP, reducing their diffusion and minimizing oxidative damage. In magnetosomes, the radicals are likely retained on the surface of the Fe_3O_4 core or confined by the lipid membrane, preventing their diffusion and contributing to an antioxidant effect by decomposing H_2O_2. Moreover, Fe_3O_4 nanozymes exhibit catalase-like activity under neutral pH conditions[146]. Given that magnetosomes are localized in the neutral cytoplasm of magnetotactic bacteria, their ROS-scavenging behavior may also involve catalase-like activity. Ferritin, a cage-shaped protein responsible for iron storage, has an iron core that exhibits SOD-like activity (Fig. 6b). Notably, the SOD-like activity of the ferritin cores in prokaryotes is higher compared to eukaryotes[42]. Modulating the expression of ferritin nanozymes in *Escherichia coli*, either by overexpression or knockout, affects the organism's tolerance to superoxide anions, underscoring its role in antioxidant defense under physiological conditions. Biogenic ferrihydrite nanoparticles, which form around fungal hyphae after interacting with hematite, function as extracellular peroxidase-like nanozymes, mitigating cytotoxicity by scavenging H_2O_2[183,184]. These studies show that nano-minerals, as natural biogenic nanozymes, are involved in the redox regulation of organisms and may have co-evolved with them. A recent study showed that condensed droplets formed by polyphosphate and Mn^{2+} ions as "protocells" protected internal nucleic acids and proteins from oxidative damage caused by high-dose radiation (1000 Gy) through their antioxidant activity[185,186]. Natural nanozymes with antioxidant properties may have played a similar role during the early stages of biological evolution, aiding early life in surviving harsh, radiation-rich environments.

In addition to inorganic minerals, some nano-assemblies formed by peptides or other biomolecules in living organisms may also have biocatalytic activity. For example, amyloid $A\beta_{1\text{-}42}$, implicated in Alzheimer's disease, forms stable nanofibrils that display peroxidase-like activity (Fig. 6c)[43]. These $A\beta_{1\text{-}42}$ nanofibrils induce increased cellular ROS levels and damage neuronal cells, suggesting that they may play a pathological role as prooxidant nanozymes in the development of Alzheimer's disease. In addition to $A\beta_{1\text{-}42}$, similar amyloid aggregates have been found in many diseases, such as islet amyloid polypeptide in type II diabetes[187], human calcitonin in thyroid cancer[188], α-synuclein in Parkinson's disease[189], and mutated SOD1 in amyotrophic lateral sclerosis[190]. These protein aggregates may also have biocatalytic activity that contributes to disease pathogenesis. More research is needed to provide evidence.

Biocatalytic applicability

Nanozymes were initially used as substitutes for enzymes in traditional enzyme applications due to their advantages in cost, stability, and versatility. For instance, referring to the application of HRP, Fe_3O_4, and other peroxidase-like nanozymes were developed for colorimetric analysis in immunoassays such as enzyme-linked immunosorbent assay (ELISA), immunohistochemistry, and test strips, and as markers in biosensors for detecting various analytes, such as glucose and H_2O_2 (Fig. 7a)[191]. With continued research, the scope of nanozyme applications has expanded beyond traditional enzymatic functions, paving the way for innovative biocatalytic strategies.

In recent years, increasing attention has been given to the in vivo applications of nanozymes for disease diagnosis and treatment. Preclinical studies have shown that many nanozymes can perform biocatalytic functions within living organisms, and there is hope to break through the application bottleneck of enzymes in disease treatment caused by the easy degradation and the induction of immune responses. Current research on in vivo applications of nanozymes primarily focuses on regulating ROS through oxidoreductase-like nanozymes to influence biological processes like metabolism, immunity, and signal transduction (Fig. 7b)[40,192]. For example, peroxidase-like or oxidase-like nanozymes such as Fe_3O_4 and Au are studied to combat tumors and bacterial infections by elevating ROS levels, mimicking the physiological effects of natural oxidases such as NADPH oxidase, xanthine oxidase, and myeloperoxidase[193]. Conversely, nanozymes with SOD-like and catalase-like activities, such as CeO_2 and Prussian blue, are being explored for their antioxidant properties to mitigate oxidative damage induced by radiation and drugs, inflammation such as enteritis and arthritis, and oxidative stress in neurological diseases such as cerebral infarction and Alzheimer's disease[194]. Beyond medical applications, antioxidant nanozymes are also being used in agriculture to improve the resistance of crops to various stresses (Fig. 7c). For example, injecting CeO_2 nanozymes with SOD-like and catalase-like activities into the leaves of Arabidopsis enhances the stress resistance by quenching ROS and improving photosynthetic efficiency[195,196].

The distinctive characteristics of nanozymes enhance their utility in biocatalytic applications, offering superior performance and expanded functionalities compared to enzymes. Some nanozymes outperform enzymes in applications due to their high single-particle or specific activity, which provides notable advantages such as accelerated reaction rates, increased efficiency, and reduced operational costs. For example, the peroxidase-like activity of a Ni–Pt nanozyme ($k_{cat} = 4.5 \times 10^7\ s^{-1}$, calculated from the single-particle concentration) is nearly 10,000 times that of HRP ($k_{cat} = 4.3 \times 10^3\ s^{-1}$). In an ELISA assay based on Ni–Pt nanozyme for detecting carcinoembryonic antigen, an ultrasensitive detection limit of 1.1 pg/mL was achieved, which is 342 times lower than the traditional HRP-ELISA (376 pg/mL)[197]. Similarly, the specific activity of the peroxidase-like activity of the PSS-modified Ru nanozyme (2820 U/mg) is nearly twice that of HRP (1305 U/mg), and the detection sensitivity of Ru-ELISA is 140 times higher than that of HRP-ELISA in detecting human alpha-fetoprotein[139].

The biocatalytic function of nanozymes is exemplified by their self-cascading catalysis, allowing them to catalyze multiple reactions within a single system, thereby simplifying catalytic pathways and enhancing overall efficiency. For example, BSA-stabilized Au nanozymes have glucose oxidase-like activity and peroxidase-like activity. These two activities are cascaded, with the former catalyzing glucose oxidation to produce H_2O_2 and the latter catalyzing H_2O_2 to produce •OH, which is used for rapid one-pot colorimetric detection of glucose[198,199]. Similarly, based on the cascade of glucose oxidase-like and peroxidase-like activities, Ru nanozymes aggravated glucose starvation and oxidative damage in U14 tumors in mice[200]. Mn_3O_4 nanozyme has SOD-like and catalase-like activities, which cascade to remove multiple reactive oxygen species such as $O_2^{\bullet-}$, H_2O_2, and •OH, and alleviated phorbol 12-myristate 13-acetate (PMA)-induced ear inflammation in mice[201].

Nanozymes have expanded the application scope of biocatalysis. On the one hand, their unique catalytic mechanisms allow for the exploration of diverse substrates and reaction types. For example, peroxidase-like nanozymes such as F_3O_4 and Fe_3S_4 catalyze the generation of •OH from H_2O_2, enabling bacterial and tumor killing, a capability not achievable with HRP. On the other hand, the robustness of nanozymes under harsh conditions extends their application to non-physiological environments. For example, the oxidase-like activity of the UoZ-4 nanozyme is stable across a wide temperature range (10 °C–100 °C), demonstrating both cold- and heat-adapted properties[202]. This feature has been used to detect the antioxidant capacity of citrus fruits at different temperatures. Cold-adapted nanozymes have been studied to block the spread of viruses through the cold chain. For example, FeN_4P_2 single-atom nanozymes exhibit lipid oxidase-like activity at cold-chain temperatures (−20 °C and 4 °C) and destroy a variety of enveloped viruses (human, porcine, and avian coronaviruses and H1–H11 subtypes of IAV) by catalyzing lipid

https://doi.org/10.1038/s41467-025-62063-8

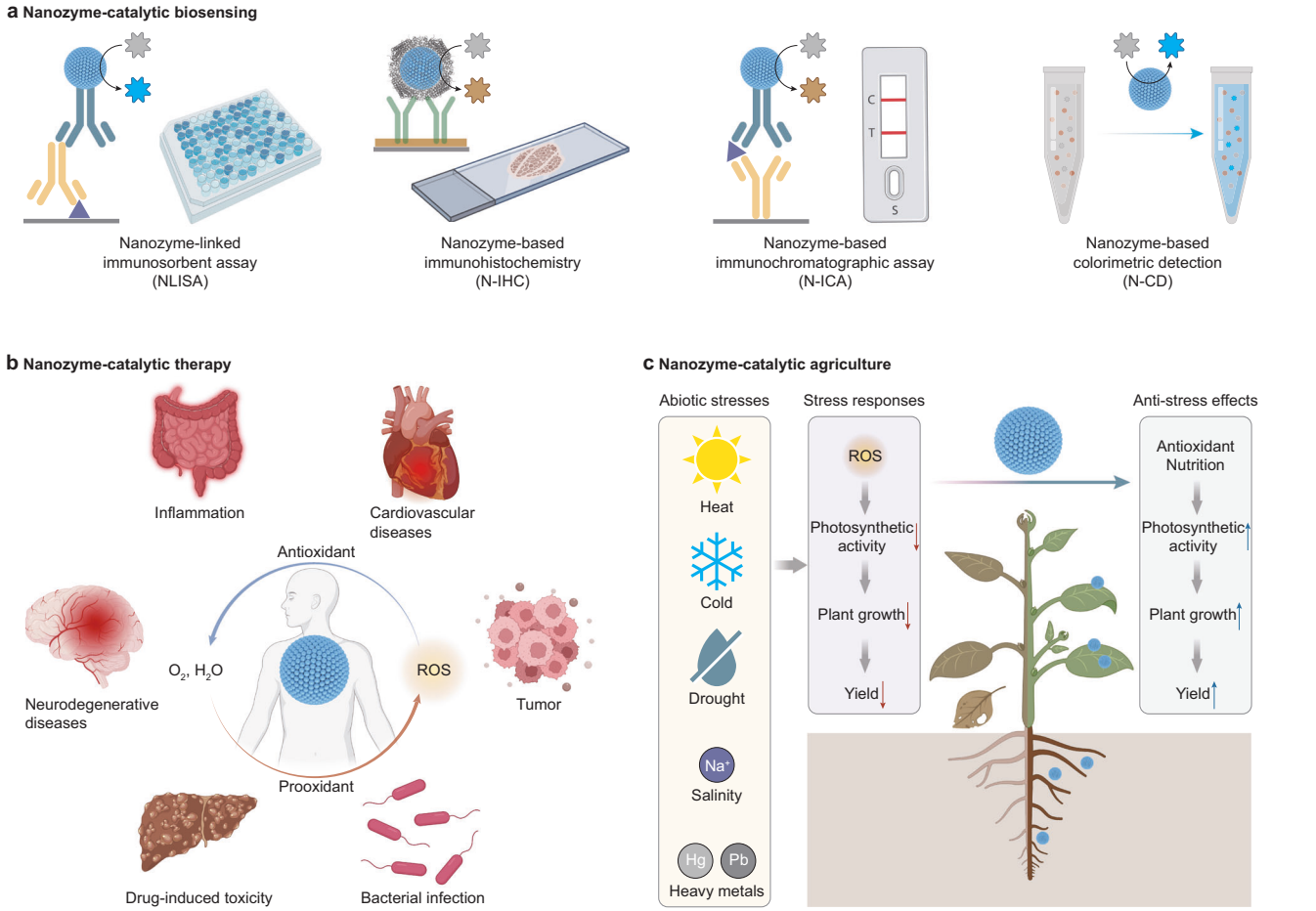

Fig. 7 | Biocatalytic applications of nanozymes. a In vitro, nanozymes are used as enzyme substitutes for biosensing, including nanozyme-based immunoadsorption, immunohistochemistry, immunochromatography, and colorimetric detection. **b** In vivo, nanozymes regulate the conversion of reactive oxygen species (ROS) for the development of antioxidant therapies targeting inflammation, drug-induced toxicity, neurodegenerative diseases, and cardiovascular diseases, as well as pro-oxidative therapies for tumors and bacterial infections. **c** Nanozymes are employed in agriculture for their antioxidant catalytic activity and as nutritional components to mitigate yield reductions caused by abiotic stresses such as heat, cold, drought, salinity, and heavy metals. (Partly created with BioRender. Zhang, R. (2025) https://BioRender.com/13q0d9v).

peroxidation of the viral lipid envelope[203]. Under simulated cold-chain logistics conditions, FeN_4P_2 single-atom nanozymes were applied to antiviral coatings on the outer packaging and personal protective equipment. Similarly, the cold-adapted nMnBTC nanozyme with oxidase-like activity showed efficient killing performance against the H1N1 influenza virus at −20 °C[157].

Nanozymes are diverse in material and easy to modify, making them versatile to combine various functional motifs for achieving diverse applications. For example, Fe_3O_4 nanozymes are synthesized inside ferritin. These nanozymes target tumor cells through the ferritin shell, while the internal Fe_3O_4 core performs peroxidase-like activity to catalyze the substrate 3,3′-diaminobenzidine (DAB) to produce brown precipitates, thereby achieving rapid and sensitive histochemical detection of tumor tissues[204]. In another example, ultra-small peroxidase-like Au nanozymes modified with neutravidin were designed for in vivo detection of tumors. After the Au nanozymes were injected into mice, the surface modification was cut off by matrix metalloproteinase-9 (MMP-9) at the tumor site, releasing free Au particles small enough to be excreted by the kidneys. In the collected urine, these Au particles catalyzed H_2O_2 and TMB to produce a color reaction through their peroxidase-like activity, allowing for tumor diagnosis through colorimetry[205]. These modifications enable targeted diagnostics and customized therapeutic approaches, highlighting the adaptability of nanozymes in diverse and specialized applications.

Some nanozymes possess unique magnetic, optical, and other physicochemical properties that, when combined with their biocatalytic activities, enable multifunctional applications. For example, Fe_3O_4 nanozymes used in ELISA not only catalyzed color development through their peroxidase-like activity but also enriched antigens through their superparamagnetism, thereby amplifying the detection signal[28]. Some nanozymes, such as Au[206], Ag[207], and Mo_2N[208] have both peroxidase-like activity and surface-enhanced Raman scattering (SERS) properties. The sensing system constructed by combining these two properties improves the sensitivity of detection of analytes such as glucose and lactic acid. For another example, the fluorescence of Cu-CDs nanozymes is quenched by hydroquinone in a concentration-dependent manner. When hydroquinone is detected by using the laccase-like activity of Cu-CDs nanozymes, high-sensitivity detection is achieved in combination with the degree of fluorescence quenching[209].

Furthermore, certain nanozymes exhibit responsiveness to external stimuli such as near-infrared light, ultrasound, and magnetic fields, enabling the development of intelligent and remote-controlled applications. For instance, liposome-encapsulated Ir nanozymes accumulate in tumors and catalyze the conversion of H_2O_2 into O_2, thereby alleviating tumor hypoxia[210]. When subjected to mild photothermal heating induced by near-infrared laser, the catalytic activity of these nanozymes was enhanced, boosting their effectiveness in alleviating hypoxia and enhancing the therapeutic outcomes of

radiotherapy on 4T1 tumor-bearing mice. In another study, near-infrared laser irradiation promoted the peroxidase-like activity of N-doped sponge-like carbon spheres, enhancing their ability to catalyze H_2O_2 into •OH to kill bacteria[211]. Ultrasound as an external signal input amplifies the peroxidase-like activity of CaF_2 nanozyme and promotes its oxidative killing effects on 4T1 breast cancer and H22 liver cancer in mice[212]. Fe_3O_4 nanozymes mineralized within a protein cage respond to alternating magnetic fields to increase temperature, enhancing their catalase-like catalytic efficiency. This capability not only alleviates hypoxia but also synergizes with magnetothermal effects to inhibit the growth of A549 subcutaneous tumors in mice and extend the survival time of mice with in situ liver cancer[213]. These remote-controlled features enable advanced therapeutic strategies and precise interventions.

Future and perspective

Research on nanozymes has advanced biocatalysis and nanomedicine, with its influence continuing to expand. Nanozymes have extended the scope of biocatalytic materials, overcoming the traditional dependence on natural enzymes for biochemical regulation and enabling catalysis in environments where enzymes are ineffective. Moreover, studies on nanozymes indicate that nanomaterials may exhibit catalytic activity in biological systems and induce notable biological effects, an aspect often overlooked in previous nanomedical applications.

Looking forward, research on nanozymes faces several promising yet complex challenges ripe for exploration. One key priority is to unravel their catalytic mechanisms and pinpoint their true active sites, tasks complicated by their heterogeneous structures and diverse active phases. Cutting-edge tools like X-ray photoelectron spectroscopy (XPS) and Fourier-transform infrared spectroscopy (FTIR) can probe atomic-level structures and chemical environments, while single-molecule and in situ techniques, such as scanning tunneling microscopy (STM) and cryo-electron microscopy (cryo-EM), enable real-time observation of catalytic processes[214,215]. Integrating these experimental approaches with computational modeling, such as density functional theory (DFT) and machine learning-based analyses, could offer deeper insights into substrate binding, transition states, and reaction pathways[69]. From a kinetic perspective, many nanozymes deviate from conventional enzymatic models due to their multi-site, multifunctional, and multi-substrate characteristics, necessitating tailored kinetic frameworks to accurately describe their catalytic behavior. Bridging theoretical tools from both heterogeneous catalysis and enzymology may be crucial for capturing their complex reaction dynamics.

Enhancing reaction specificity is another critical aspect for advancing nanozyme applications, as it improves catalytic efficiency while minimizing undesired side reactions. Achieving this requires a detailed understanding of the structure–activity relationship between active site microstructures and their catalytic pathways[114]. When specific active sites with well-defined coordination and electronic structures dominate, the catalytic pathways of nanozymes may exhibit enhanced specificity[122,216]. Additionally, cascade reactions involving multiple nanozymes can progressively screen substrates to improve overall reaction selectivity[155]. While specificity is essential, the broad substrate interaction spectrum of nanozymes also presents unique advantages. For example, porphyrin-like Fe-N-C nanozymes demonstrate enzyme-like behaviors akin to cytochrome P450 enzymes, accelerating drug metabolism and exhibiting drug inhibition[217]. These behaviors arise from broad interactions between the heme-like $Fe–N_x$ coordination centers and diverse substrates. Exploiting this property enables the development of rapid, cost-effective platforms for analyzing drug-drug interactions, which guide therapeutic decisions and predict in vivo outcomes[88]. Moreover, the multifunctionality of nanozymes parallels that of primordial enzymes, which likely supported early biological evolution by performing diverse functions with a limited enzyme repertoire. This characteristic makes nanozymes valuable models for exploring primitive life-like processes[218].

The range of nanozyme materials and their catalytic functions is projected to keep diversifying (Box 2). Inorganic materials currently lead the field, but research is increasingly investigating a broader array of nanomaterials, including inorganic, organic, or mixed (organometallic) structures with inherent biocatalytic properties. For example, iron-anchored β-lactoglobulin amyloid fibrils display peroxidase-like activity and degrade alcohol in the gastrointestinal tract following oral intake[219]. Despite being protein-based, their nanofiber structure with abundant anchored iron sites qualifies them as nanozymes. This diversification of material types is expected to expand the catalytic repertoire of nanozymes, facilitating the development of catalysts capable of performing complex biocatalytic functions. While oxidoreductase-like activity remains the primary focus of nanozyme research, other catalytic functions, including hydrolase-like, isomerase-like, and lyase-like activities, have also been demonstrated, with some nanozymes even catalyzing reactions in biological systems that natural enzymes cannot (Box 2). To further expand functionality, strategies could involve exploring alternative materials that offer tunable structures and diverse active sites, such as MOFs, COFs, or hybrid materials combining organic and inorganic components. Another approach is to rationally design nanozymes that mimic the active sites of hydrolases, isomerases, or lyases by incorporating functional groups or cofactors.

The integration of high-throughput computing with materials science has advanced the design and prediction of nanozymes. Using first-principles calculations, like DFT, researchers can predict the electronic and thermodynamic properties at the atomic level[69]. High-throughput computing leverages parallel processing to rapidly analyze large datasets, facilitating the identification of nanostructures with enhanced catalytic performance, and accelerating material screening while reducing experimental trial-and-error[220]. Machine learning is also becoming more important in nanozyme research. By analyzing experimental and computational data, it can uncover key structure–activity relationships, predict catalytic performance, and guide experimental design[221,222]. For example, machine learning has been used to predict how different doping elements affect the peroxidase-like activity of graphdiyne-based nanozymes, expediting discovery and optimization[223]. As research on nanozymes generates larger datasets, the potential of big data analytics and machine learning in accelerating the development of high-performance nanozymes becomes even more evident. However, all these computing tools have their respective strengths and limitations, and relying solely on one may not fully address the complexity of nanozyme design. For instance, as nanozyme-catalyzed reactions are often influenced by external field environments, relying solely on DFT-guided thermodynamic analysis is insufficient to fully elucidate their mechanisms, requiring integration with kinetic analysis derived from experimentally validated data or molecular simulations[222]. Therefore, the next stage of research could focus on integrating different computational and data-driven methods to establish more realistic and accurate models for describing and predicting nanozyme behavior.

The discovery of natural nanozymes, such as magnetosomes[41], ferritin[42], and Aβ amyloid protein aggregates[43], indicates that nanozymes are not limited to synthetic materials but may also play physiological and pathological roles as natural biocatalysts. Natural inorganic nanomaterials are widespread, found both globally and within organisms, indicating that many other natural nanozymes likely remain to be discovered. Advances in the characterization of intracellular inorganic particles and related technologies offer promising avenues for uncovering the diversity of natural nanozymes and understanding their roles in biological processes. Furthermore, exploring whether natural nanozymes represent a primordial form of

biocatalysts and investigating their evolutionary significance to early life and primitive enzymes presents an exciting area for future research[44].

Research on nanozymes in living organisms is expected to progress further, with promising applications in addressing redox imbalances, metabolic disorders, and immune dysfunctions. Moreover, progress in nanozyme-based medical research has led to the discovery of unique interactions between nanomaterials and biological systems, such as the specific transcytosis of chiral MOF nanomaterials[224] and ferroptosis-like death in bacteria induced by FeS_2 nanozymes[225]. However, challenges remain for in vivo applications and clinical translation. The in vivo environment presents distinct hurdles, including heterogeneous microenvironments, variable pH, ionic strength, and the presence of competing biomolecules, all of which substantially impact the activity and stability of nanozymes. These factors often result in discrepancies between in vitro findings and in vivo performance. Addressing these challenges requires examining nanozyme behavior under physiologically relevant conditions and assessing their catalytic activity, stability, and substrate specificity in the presence of complex cellular components like proteins, lipids, and nucleic acids. Advanced techniques, including fluorescence resonance energy transfer (FRET), in situ Raman spectroscopy, X-ray imaging, and mass spectrometry, could provide valuable insights by enabling real-time monitoring of nanozyme activity and substrate interactions in living systems[226–228]. While preliminary studies suggest many nanozymes exhibit good biocompatibility, their in vivo effects remain largely unpredictable, necessitating further investigation into potential toxicity and long-term side effects. Future research could prioritize the design of nanozymes with enhanced adaptability, such as responsiveness to specific microenvironmental factors like pH or redox conditions, to improve both their catalytic efficiency and biosafety. However, it is crucial to strike a balance between material functionality and complexity. Materials with greater functionality often exhibit more complex structures, which complicate their clinical translation. Additionally, there is an urgent need to develop efficient and controllable synthesis methods, stable formulations, and targeted delivery strategies to ensure consistent performance in in vivo applications.

Finally, understanding the biocatalytic activity of nanozymes under extreme conditions is an important avenue for future research. Nanozymes capable of catalyzing reactions in extreme environments could provide insights into the survival strategies of extremophiles and early evolutionary organisms, which rely on catalytic processes for antioxidant functions, metabolism, and energy transport[44]. These nanozymes could be used in a broader range of applications compared to natural enzymes. For instance, thermostable nanozymes could be valuable in high-temperature environments such as chemical synthesis, food processing, and textiles. Cold-adapted nanozymes may be useful in low-temperature applications like food refrigeration, cold chain disinfection, and environmental management in polar regions. Salt-tolerant nanozymes could be applied in high-salinity environments such as salted food processing and marine environmental management. To achieve this, it is essential to investigate the types of materials and biocatalytic activities of nanozymes that function under extreme conditions and to elucidate their catalytic mechanisms to guide the design of materials better suited for these applications.

References

1. Kirk, O., Borchert, T. V. & Fuglsang, C. C. Industrial enzyme applications. *Curr. Opin. Biotechnol.* **13**, 345–351 (2002).
2. Payen, A. & Persoz, J. F. Memoir on diastase, the principal products of its reactions, and their applications to the industrial arts. *Ann. Chim. Phys.* **53**, 73–92 (1833).
3. Nelson, J. M. Enzymes from the standpoint of the chemistry of invertase. *Chem. Rev.* **12**, 1–42 (1933).
4. Fruton, J. osephS. A history of pepsin and related enzymes. *Q. Rev. Biol.* **77**, 127–147 (2002).
5. Theorell, H. Nature and mode of action of oxidation enzymes. *Science* **124**, 467–472 (1956).
6. Kuhne, W. Über das Verhalten verschiedener organisirter und sog. ungeformter Fermente. *Verh. Naturhistorisch Med. Ver. Zu Heidelber* **1**, 190–193 (1877).
7. Barnett, J. A. A history of research on yeasts 2: Louis Pasteur and his contemporaries, 1850–1880. *Yeast* **16**, 755–771 (2000).
8. Buchner, E. Alkoholische gährung ohne hefezellen. *Ber. Dtsch. Chem. Ges.* **30**, 117–124 (1897).
9. Sumner, J. B. In *A Source Book in Chemistry, 1900-1950* (ed. Leicester, H. M.) 322–327 (Harvard University Press, 1968).
10. Manchester, K. L. The crystallization of enzymes and virus proteins: laying to rest the colloidal concept of living systems. *Endeavour* **28**, 25–29 (2004).
11. Kruger, K. et al. Self-splicing RNA: autoexcision and autocyclization of the ribosomal RNA intervening sequence of tetrahymena. *Cell* **31**, 147–157 (1982).
12. Sellami-Kamoun, A. et al. Stability of thermostable alkaline protease from Bacillus licheniformis RP1 in commercial solid laundry detergent formulations. *Microbiol. Res.* **163**, 299–306 (2008).
13. Garg, S. K. & Johri, B. N. Rennet: current trends and future research. *Food Rev. Int.* **10**, 313–355 (1994).
14. Kang, C. K. & Warner, W. D. Tenderization of meat with papaya latex proteases. *J. Food Sci.* **39**, 812–818 (1974).
15. Yoo, Y. J., Feng, Y. & Yagonia, C. F. J. *Fundamentals of Enzyme Engineering* (Springer, 2017).
16. DeSantis, G. & Jones, J. B. Chemical modification of enzymes for enhanced functionality. *Curr. Opin. Biotechnol.* **10**, 324–330 (1999).
17. Demain, A. L. & Vaishnav, P. Production of recombinant proteins by microbes and higher organisms. *Biotechnol. Adv.* **27**, 297–306 (2009).
18. Arnold, F. H. Design by directed evolution. *Acc. Chem. Res.* **31**, 125–131 (1998).
19. Chen, K. & Arnold, F. H. Tuning the activity of an enzyme for unusual environments: sequential random mutagenesis of subtilisin E for catalysis in dimethylformamide. *Proc. Natl. Acad. Sci. USA* **90**, 5618–5622 (1993).
20. Coelho, P. S., Brustad, E. M., Kannan, A. & Arnold, F. H. Olefin cyclopropanation via carbene transfer catalyzed by engineered cytochrome P450 enzymes. *Science* **339**, 307–310 (2013).
21. Prier, C. K., Hyster, T. K., Farwell, C. C., Huang, A. & Arnold, F. H. Asymmetric enzymatic synthesis of allylic amines: a sigmatropic rearrangement strategy. *Angew. Chem. Int. Ed.* **55**, 4711–4715 (2016).
22. Breslow, R. & Overman, L. E. "Artificial enzyme" combining a metal catalytic group and a hydrophobic binding cavity. *J. Am. Chem. Soc.* **92**, 1075–1077 (1970).
23. Murakami, Y., Kikuchi, J. I., Hisaeda, Y. & Hayashida, O. Artificial enzymes. *Chem. Rev.* **96**, 721–758 (1996).
24. Wulff, G. Enzyme-like catalysis by molecularly imprinted polymers. *Chem. Rev.* **102**, 1–28 (2002).
25. Slama, J. T., Oruganti, S. R. & Kaiser, E. T. Semisynthetic enzymes: synthesis of a new flavopapain with high catalytic efficiency. *J. Am. Chem. Soc.* **103**, 6211–6213 (1981).
26. Santoro, S. W. & Joyce, G. F. A general purpose RNA-cleaving DNA enzyme. *Proc. Natl. Acad. Sci. USA* **94**, 4262–4266 (1997).
27. Tramontano, A., Janda, K. D. & Lerner, R. A. Catalytic antibodies. *Science* **234**, 1566–1570 (1986).
28. Gao, L. et al. Intrinsic peroxidase-like activity of ferromagnetic nanoparticles. *Nat. Nanotechnol.* **2**, 577–583 (2007). This article reports that ferromagnetic nanoparticles possess intrinsic peroxidase-like activity and establishes a paradigm for

characterizing the biocatalytic properties of nanomaterials using enzymatic methods.
29. Wei, H. & Wang, E. Nanomaterials with enzyme-like characteristics (nanozymes): next-generation artificial enzymes. *Chem. Soc. Rev.* **42**, 6060–6093 (2013). This article provides a comprehensive overview of early research progress on nanozymes.
30. Wu, J. et al. Nanomaterials with enzyme-like characteristics (nanozymes): next-generation artificial enzymes (II). *Chem. Soc. Rev.* **48**, 1004–1076 (2019).
31. Wang, Z., Zhang, R., Yan, X. & Fan, K. Structure and activity of nanozymes: inspirations for de novo design of nanozymes. *Mater. Today* **41**, 81–119 (2020). This article reviews studies on the structure–activity relationship of nanozymes, underscoring how nanostructural features influence their biocatalytic properties.
32. Li, S. et al. Data-informed discovery of hydrolytic nanozymes. *Nat. Commun.* **13**, 827 (2022).
33. Chen, J. et al. Bio-inspired nanozyme: a hydratase mimic in a zeolitic imidazolate framework. *Nanoscale* **11**, 5960–5966 (2019).
34. Li, F. et al. Chiral carbon dots mimicking topoisomerase I to mediate the topological rearrangement of supercoiled DNA enantioselectively. *Angew. Chem. Int. Ed.* **59**, 11087–11092 (2020).
35. Sheng, J. et al. Multienzyme-like nanozymes: regulation, rational design, and application. *Adv. Mater.* **36**, 2211210 (2024).
36. Jiang, D. et al. Nanozyme: new horizons for responsive biomedical applications. *Chem. Soc. Rev.* **48**, 3683–3704 (2019).
37. Alizadeh, N. & Salimi, A. Multienzymes activity of metals and metal oxide nanomaterials: applications from biotechnology to medicine and environmental engineering. *J. Nanobiotechnol.* **19**, 26 (2021).
38. Zhao, L. et al. Nanobiotechnology-based strategies for enhanced crop stress resilience. *Nat. Food* **3**, 829–836 (2022).
39. Dong, H., Fan, Y., Zhang, W., Gu, N. & Zhang, Y. Catalytic mechanisms of nanozymes and their applications in biomedicine. *Bioconjugate Chem.* **30**, 1273–1296 (2019).
40. Zhang, R., Jiang, B., Fan, K., Gao, L. & Yan, X. Designing nanozymes for in vivo applications. *Nat. Rev. Bioeng.* **2**, 849–868 (2024). This article summarizes design criteria for nanozymes in in vivo applications and highlights opportunities and challenges in nanozyme-driven biocatalytic medicine.
41. Guo, F. F. et al. Magnetosomes eliminate intracellular reactive oxygen species in Magnetospirillum gryphiswaldense MSR-1. *Environ. Microbiol.* **14**, 1722–1729 (2012).
42. Ma, L. et al. A natural biogenic nanozyme for scavenging superoxide radicals. *Nat. Commun.* **15**, 233 (2024). This article reports the ferric core of ferritin as a natural nanozyme with superoxide dismutase-like activity and reveals an evolutionary decline of this catalytic function across species.
43. Yuan, Y. et al. Histidine modulates amyloid-like assembly of peptide nanomaterials and confers enzyme-like activity. *Nat. Commun.* **14**, 5808 (2023).
44. Ma, L. et al. Nanozymes and their potential roles in the origin of life. *Adv. Mater.* **37**, 2412211 (2025).
45. Manea, F., Houillon, F. B., Pasquato, L. & Scrimin, P. Nanozymes: gold-nanoparticle-based transphosphorylation catalysts. *Angew. Chem. Int. Ed.* **43**, 6165–6169 (2004).
46. Pluth, M. D., Bergman, R. G. & Raymond, K. N. Catalytic deprotection of acetals in basic solution with a self-assembled supramolecular "nanozyme". *Angew. Chem. Int. Ed.* **46**, 8587–8589 (2007).
47. Batrakova, E. V. et al. A macrophage–nanozyme delivery system for Parkinson's disease. *Bioconjugate Chem.* **18**, 1498–1506 (2007).
48. Scott, S., Zhao, H., Dey, A. & Gunnoe, T. B. Nano-apples and orange-zymes. *ACS Catal.* **10**, 14315–14317 (2020).
49. Robert, A. & Meunier, B. How to define a nanozyme. *ACS Nano* **16**, 6956–6959 (2022).
50. Lyu, Y. & Scrimin, P. Mimicking enzymes: the quest for powerful catalysts from simple molecules to nanozymes. *ACS Catal.* **11**, 11501–11509 (2021).
51. Wang, Q., Wei, H., Zhang, Z., Wang, E. & Dong, S. Nanozyme: an emerging alternative to natural enzyme for biosensing and immunoassay. *TrAC Trends Anal. Chem.* **105**, 218–224 (2018).
52. Zandieh, M. & Liu, J. Nanozymes: definition, activity, and mechanisms. *Adv. Mater.* **36**, 2211041 (2024).
53. Dong, H. et al. Depletable peroxidase-like activity of Fe_3O_4 nanozymes accompanied with separate migration of electrons and iron ions. *Nat. Commun.* **13**, 5365 (2022). This article reports that internal atoms of Fe_3O_4 nanozymes participate in peroxidase-like catalysis through electron transfer to the surface.
54. Wan, K., Jiang, B., Tan, T., Wang, H. & Liang, M. Surface-mediated production of complexed •OH radicals and Fe=O species as a mechanism for iron oxide peroxidase-like nanozymes. *Small* **18**, 2204372 (2022).
55. Berglund, G. I. et al. The catalytic pathway of horseradish peroxidase at high resolution. *Nature* **417**, 463–468 (2002).
56. Josephy, P. D., Eling, T. & Mason, R. P. The horseradish peroxidase-catalyzed oxidation of 3,5,3',5'-tetramethylbenzidine. Free radical and charge-transfer complex intermediates. *J. Biol. Chem.* **257**, 3669–3675 (1982).
57. Mozaffar, S. et al. Properties of catalase purified from a methanol-grown yeast, Kloeckera sp. 2201. *Eur. J. Biochem.* **155**, 527–531 (1986).
58. Xu, J. et al. Tumor microenvironment-responsive mesoporous MnO_2-coated upconversion nanoplatform for self-enhanced tumor theranostics. *Adv. Funct. Mater.* **28**, 1803804 (2018).
59. Berg, J. M., Tymoczko, J. L. & Stryer, L. *Biochemistry (Loose-Leaf)* (Macmillan, 2007).
60. Creighton, T. E. *Proteins: Structures and Molecular Properties* (Macmillan, 1993).
61. Cao, X. et al. Insight into iron leaching from an ascorbate-oxidase-like Fe–N–C nanozyme and oxygen reduction selectivity. *Angew. Chem. Int. Ed.* **135**, e202302463 (2023).
62. Lu, X. et al. Bridging oxidase catalysis and oxygen reduction electrocatalysis by model single-atom catalysts. *Natl. Sci. Rev.* **9**, nwac022 (2022).
63. Hernández-Ruiz, J., Arnao, M. B., Hiner, A. N. P., García-Cánovas, F. & Acosta, M. Catalase-like activity of horseradish peroxidase: relationship to enzyme inactivation by H_2O_2. *Biochem. J.* **354**, 107–114 (2001).
64. Goldstein, I. et al. Chemotherapeutic agents induce the expression and activity of their clearing enzyme CYP3A4 by activating p53. *Carcinogenesis* **34**, 190–198 (2012).
65. Zhang, Z., Zhang, X., Liu, B. & Liu, J. Molecular imprinting on inorganic nanozymes for hundred-fold enzyme specificity. *J. Am. Chem. Soc.* **139**, 5412–5419 (2017). This article reports that the substrate specificity of the peroxidase-like activity of Fe_3O_4 nanozyme is increased by nearly 100-fold by constructing substrate-specific recognition sites on the periphery of the nanozyme using a molecular imprinting method.
66. Zhang, R., Zhou, Y., Yan, X. & Fan, K. Advances in chiral nanozymes: a review. *Microchim. Acta* **186**, 782 (2019).
67. Somerville, S. V. et al. Approaches to improving the selectivity of nanozymes. *Adv. Mater.* **36**, 2211288 (2024).
68. Chen, X. et al. Bound oxygen-atom transfer endows peroxidase-mimic M–N–C with high substrate selectivity. *Chem. Sci.* **12**, 8865–8871 (2021).
69. Shen, X., Wang, Z., Gao, X. J. & Gao, X. Reaction mechanisms and kinetics of nanozymes: insights from theory and computation. *Adv. Mater.* **36**, 2211151 (2024).

70. Gao, L., Gao, X. & Yan, X. In *Nanozymology: Connecting Biology and Nanotechnology* (ed. Yan, X.) 17–39 (Springer Singapore, 2020).
71. Srinivasan, B. A guide to the Michaelis–Menten equation: steady state and beyond. *FEBS J.* **289**, 6086–6098 (2022).
72. Jiang, B. et al. Standardized assays for determining the catalytic activity and kinetics of peroxidase-like nanozymes. *Nat. Protoc.* **13**, 1506–1520 (2018).
73. Panferov, V. G., Zhang, W., D'Abruzzo, N., Wang, S. & Liu, J. Kinetic profiling of oxidoreductase-mimicking nanozymes: impact of multiple activities, chemical transformations, and colloidal stability. *ACS Nano* **18**, 34870–34883 (2024).
74. Johnson, K. A. & Goody, R. S. The original Michaelis constant: translation of the 1913 Michaelis–Menten paper. *Biochemistry* **50**, 8264–8269 (2011).
75. Zhang, M., Wang, M., Xu, B. & Ma, D. How to measure the reaction performance of heterogeneous catalytic reactions reliably. *Joule* **3**, 2876–2883 (2019).
76. Zhang, R. et al. Edge-site engineering of defective Fe–N_4 nanozymes with boosted catalase-like performance for retinal vasculopathies. *Adv. Mater.* **34**, 2205324 (2022).
77. Seibert, E. & Tracy, T. S. In *Enzyme Kinetics in Drug Metabolism: Fundamentals and Applications* (eds Nagar, S., Argikar, U. A. & Tweedie, D.) 3–27 (Springer US, 2021).
78. Klotz, I. M. & Hunston, D. L. Properties of graphical representations of multiple classes of binding sites. *Biochemistry* **10**, 3065–3069 (1971).
79. Bull, C. & Fee, J. A. Steady-state kinetic studies of superoxide dismutases: properties of the iron containing protein from Escherichia coli. *J. Am. Chem. Soc.* **107**, 3295–3304 (1985).
80. Zaupa, G., Scrimin, P. & Prins, L. J. Origin of the dendritic effect in multivalent enzyme-like catalysts. *J. Am. Chem. Soc.* **130**, 5699–5709 (2008).
81. Zaupa, G., Mora, C., Bonomi, R., Prins, L. J. & Scrimin, P. Catalytic self-assembled monolayers on Au nanoparticles: the source of catalysis of a transphosphorylation reaction. *Chem. Eur. J.* **17**, 4879–4889 (2011).
82. Wang, Y., Li, T. & Wei, H. Determination of the maximum velocity of a peroxidase-like nanozyme. *Anal. Chem.* **95**, 10105–10109 (2023).
83. Zandieh, M. & Liu, J. Nanozyme catalytic turnover and self-limited reactions. *ACS Nano* **15**, 15645–15655 (2021).
84. Ji, S. et al. Matching the kinetics of natural enzymes with a single-atom iron nanozyme. *Nat. Catal.* **4**, 407–417 (2021). This article reports that single-atom nanozymes with FeN_3P active centers coordinate phosphorus and nitrogen to modulate the electronic structure of iron, achieving catalytic activity and kinetics comparable to natural enzymes.
85. Huang, L., Chen, J., Gan, L., Wang, J. & Dong, S. Single-atom nanozymes. *Sci. Adv.* **5**, eaav5490 (2019).
86. Fan, K. et al. In vivo guiding nitrogen-doped carbon nanozyme for tumor catalytic therapy. *Nat. Commun.* **9**, 1440 (2018). This article reports that nitrogen-doped carbon nanozymes with multiple enzyme-like activities (oxidase, peroxidase, catalase, and superoxide dismutase) selectively target and oxidatively kill tumor cells in a pH-dependent manner.
87. Li, B. et al. Diatomic iron nanozyme with lipoxidase-like activity for efficient inactivation of enveloped virus. *Nat. Commun.* **14**, 7312 (2023).
88. Wang, Y. et al. Spatial engineering of single-atom Fe adjacent to Cu-assisted nanozymes for biomimetic O_2 activation. *Nat. Commun.* **15**, 2239 (2024).
89. Zeng, R. et al. Atomically site synergistic effects of dual-atom nanozyme enhances peroxidase-like properties. *Nano Lett.* **23**, 6073–6080 (2023).
90. Park, C. Visual interpretation of the meaning of k_{cat}/K_M in enzyme kinetics. *J. Chem. Educ.* **99**, 2556–2562 (2022).
91. Spivey, J. J. et al. in *Catalysis* Vol. 17 (eds Spivey, J. J. & Roberts, G. W.) (The Royal Society of Chemistry, 2004).
92. Northrop, D. B. On the meaning of K_m and V/K in enzyme kinetics. *J. Chem. Educ.* **75**, 1153 (1998).
93. Carrillo, N., Ceccarelli, E. A. & Roveri, O. A. Usefulness of kinetic enzyme parameters in biotechnological practice. *Biotechnol. Genet. Eng. Rev.* **27**, 367–382 (2010).
94. Eisenthal, R., Danson, M. J. & Hough, D. W. Catalytic efficiency and k_{cat}/K_M: a useful comparator?. *Trends Biotechnol.* **25**, 247–249 (2007).
95. Leskovac, V. Kinetic analysis of bisubstrate mechanisms. In *Comprehensive Enzyme Kinetics* 171–189 (Springer US, 2003).
96. Jain, V., Bhagat, S., Singh, M., Bansal, V. & Singh, S. Unveiling the effect of 11-MUA coating on biocompatibility and catalytic activity of a gold-core cerium oxide-shell-based nanozyme. *RSC Adv.* **9**, 33195–33206 (2019).
97. Eadie, G. S. The inhibition of cholinesterase by physostigmine and prostigmine. *J. Biol. Chem.* **146**, 85–93 (1942).
98. Ali, S. et al. Intrinsic light-activated oxidase mimicking activity of conductive polyaniline nanofibers: a class of metal-free nanozyme. *ACS Appl. Bio Mater.* **5**, 5518–5531 (2022).
99. Aghayan, M. et al. Fe(III) porphyrin metal–organic framework as an artificial enzyme mimics and its application in biosensing of glucose and H_2O_2. *J. Porous Mater.* **26**, 1507–1521 (2019).
100. Basak, S., Sikdar, S., Ali, S., Mondal, M. & Roy, M. N. Green synthesized copper assisted iron oxide nanozyme for the efficient elimination of industrial pollutant via peroxodisulfate activation. *J. Mol. Struct.* **1283**, 135267 (2023).
101. Korzekwa, K. R. et al. evaluation of atypical cytochrome P450 kinetics with two-substrate models: evidence that multiple substrates can simultaneously bind to cytochrome P450 active sites. *Biochemistry* **37**, 4137–4147 (1998).
102. SHOU, M. et al. Sigmoidal kinetic model for two co-operative substrate-binding sites in a cytochrome P450 3A4 active site: an example of the metabolism of diazepam and its derivatives. *Biochem. J.* **340**, 845–853 (1999).
103. Ragg, R. et al. Molybdenum trioxide nanoparticles with intrinsic sulfite oxidase activity. *ACS Nano* **8**, 5182–5189 (2014).
104. Morajkar, R. V., Fatrekar, A. P. & Vernekar, A. A. Approach of a small protein to the biomimetic bis-(μ-oxo) dicopper active-site installed in MOF-808 pores with restricted access perturbs substrate selectivity of oxidase nanozyme. *Chem. Sci.* **15**, 10810–10822 (2024).
105. Derry, P. J. et al. Catalytic oxidation and reduction reactions of hydrophilic carbon clusters with NADH and cytochrome c: features of an electron transport nanozyme. *Nanoscale* **11**, 10791–10807 (2019).
106. Tracy, T. S. & Hummel, M. A. Modeling kinetic data from in vitro drug metabolism enzyme experiments. *Drug Metab. Rev.* **36**, 231–242 (2004).
107. Liang, M. & Yan, X. Nanozymes: from new concepts, mechanisms, and standards to applications. *Acc. Chem. Res.* **52**, 2190–2200 (2019).
108. Cuatrecasas, P., Wilchek, M. & Anfinsen, C. B. Selective enzyme purification by affinity chromatography. *Proc. Natl. Acad. Sci. USA* **61**, 636–643 (1968).
109. He, S. et al. Peptide nanozymes: an emerging direction for functional enzyme mimics. *Bioact. Mater.* **42**, 284–298 (2024).
110. Shen, X. et al. Mechanisms of oxidase and superoxide dismutation-like activities of gold, silver, platinum, and palladium, and their alloys: a general way to the activation of molecular oxygen. *J. Am. Chem. Soc.* **137**, 15882–15891 (2015).

111. Liu, Q., Zhang, A., Wang, R., Zhang, Q. & Cui, D. A review on metal- and metal oxide-based nanozymes: properties, mechanisms, and applications. *Nano Micro Lett.* **13**, 154 (2021).
112. Gao, W. et al. Deciphering the catalytic mechanism of superoxide dismutase activity of carbon dot nanozyme. *Nat. Commun.* **14**, 160 (2023). This article analyzes the superoxide dismutase-like catalytic mechanism of carbon dot nanozymes and reveals the role of surface-abundant oxygen-containing functional groups, such as carbonyl, carboxyl, and hydroxyl, as substrate binding or catalytic sites.
113. Niu, X. et al. Metal–organic framework based nanozymes: promising materials for biochemical analysis. *Chem. Commun.* **56**, 11338–11353 (2020).
114. Xu, Y. et al. Molecular insights of nanozymes from design to catalytic mechanism. *Sci. China Chem.* **66**, 1318–1335 (2023).
115. Veitch, N. C. Horseradish peroxidase: a modern view of a classic enzyme. *Phytochemistry* **65**, 249–259 (2004).
116. Rodríguez-López, J. N. et al. Mechanism of reaction of hydrogen peroxide with horseradish peroxidase: identification of intermediates in the catalytic cycle. *J. Am. Chem. Soc.* **123**, 11838–11847 (2001).
117. Hsueh, C. L., Huang, Y. H., Wang, C. C. & Chen, C. Y. Degradation of azo dyes using low iron concentration of Fenton and Fenton-like system. *Chemosphere* **58**, 1409–1414 (2005).
118. Gao, L., Fan, K. & Yan, X. Iron oxide nanozyme: a multifunctional enzyme mimetic for biomedical applications. *Theranostics* **7**, 3207–3227 (2017).
119. Feng, K. et al. Elucidating the catalytic mechanism of Prussian blue nanozymes with self-increasing catalytic activity. *Nat. Commun.* **15**, 5908 (2024). This article reports that Prussian blue nanozymes possess self-enhancing peroxidase-like activity, mediated by dual conduction/valence band electron transfer pathways, and irreversible surface pre-oxidation facilitates the catalytic process.
120. Singh, N., Savanur, M. A., Srivastava, S., D'Silva, P. & Mugesh, G. A redox modulatory Mn_3O_4 nanozyme with multi-enzyme activity provides efficient cytoprotection to human cells in a Parkinson's disease model. *Angew. Chem. Int. Ed.* **129**, 14455–14459 (2017).
121. Ghosh, S., Roy, P., Karmodak, N., Jemmis, E. D. & Mugesh, G. Nanoisozymes: crystal-facet-dependent enzyme-mimetic activity of V_2O_5 nanomaterials. *Angew. Chem. Int. Ed.* **130**, 4600–4605 (2018).
122. Yuan, B. et al. Regulating the H_2O_2 activation pathway on a well-defined CeO_2 nanozyme allows the entire steering of its specificity between associated enzymatic reactions. *ACS Nano* **17**, 17383–17393 (2023).
123. Jiang, L. et al. Improved oxidase mimetic activity by praseodymium incorporation into ceria nanocubes. *ACS Appl. Mater. Interfaces* **9**, 18595–18608 (2017).
124. Dang, Y. et al. Rational construction of a Ni/$CoMoO_4$ heterostructure with strong Ni–O–Co bonds for improving multifunctional nanozyme activity. *ACS Nano* **16**, 4536–4550 (2022).
125. Zhang, R., Fan, K. & Yan, X. Nanozymes: created by learning from nature. *Sci. China Life Sci.* **63**, 1183–1200 (2020).
126. Xu, Y. et al. Regulating reactive oxygen intermediates of Fe–N–C SAzyme via second-shell coordination for selective aerobic oxidation reactions. *Angew. Chem. Int. Ed.* **136**, e202408935 (2024).
127. Liu, B. & Liu, J. Surface modification of nanozymes. *Nano Res.* **10**, 1125–1148 (2017).
128. Fan, K. et al. Optimization of Fe_3O_4 nanozyme activity via single amino acid modification mimicking an enzyme active site. *Chem. Commun.* **53**, 424–427 (2017).
129. Cai, R. et al. Improving peroxidase activity of gold nanorod nanozymes by dragging substrates to the catalysis sites via cysteine modification. *Nanotechnology* **32**, https://doi.org/10.1088/1361-6528/ac1e53 (2021).
130. Liu, B., Huang, Z. & Liu, J. Boosting the oxidase mimicking activity of nanoceria by fluoride capping: rivaling protein enzymes and ultrasensitive F(-) detection. *Nanoscale* **8**, 13562–13567 (2016).
131. Sun, Y., Zhao, C., Gao, N., Ren, J. & Qu, X. Stereoselective nanozyme based on ceria nanoparticles engineered with amino acids. *Chem. Eur. J.* **23**, 18146–18150 (2017).
132. Shen, X., Wang, Z., Gao, X. & Zhao, Y. Density functional theory-based method to predict the activities of nanomaterials as peroxidase mimics. *ACS Catal.* **10**, 12657–12665 (2020).
133. Wang, X. et al. e_g occupancy as an effective descriptor for the catalytic activity of perovskite oxide-based peroxidase mimics. *Nat. Commun.* **10**, 704 (2019).
134. Wan, K., Wang, H. & Shi, X. Machine learning-accelerated high-throughput computational screening: unveiling bimetallic nanoparticles with peroxidase-like activity. *ACS Nano* **18**, 12367–12376 (2024).
135. Zhang, C. et al. Machine learning guided discovery of superoxide dismutase nanozymes for androgenetic alopecia. *Nano Lett.* **22**, 8592–8600 (2022). This article reports the machine learning-guided discovery of a superoxide dismutase-like nanozyme, $MnPS_3$, which demonstrates therapeutic efficacy against androgenetic alopecia in a mouse model.
136. Baldwin, R. L. Structure and mechanism in protein science. a guide to enzyme catalysis and protein folding, by A. Fersht. 1999. New York: Freeman. 631 pp. $67.95 (hardcover). *Protein Sci.* **9**, 207–207 (2000).
137. Zhang, R., Yan, X. & Fan, K. Nanozymes inspired by natural enzymes. *Acc. Mater. Res.* **2**, 534–547 (2021).
138. Cursi, L., Mirra, G., Boselli, L. & Pompa, P. P. Metrology of platinum nanozymes: mechanistic insights and analytical issues. *Adv. Funct. Mater.* **34**, 2315587 (2024). This article delivers a metrological analysis of platinum nanozymes, elucidating their redox enzyme-like activities under diverse conditions and establishing methodological guidelines for nanozyme characterization.
139. Fan, H. et al. Surface ligand engineering ruthenium nanozyme superior to horseradish peroxidase for enhanced immunoassay. *Adv. Mater.* **36**, 2300387 (2024).
140. Korsvik, C., Patil, S., Seal, S. & Self, W. T. Superoxide dismutase mimetic properties exhibited by vacancy engineered ceria nanoparticles. *Chem. Commun.* **10**, 1056–1058 (2007).
141. Pirmohamed, T. et al. Nanoceria exhibit redox state-dependent catalase mimetic activity. *Chem. Commun.* **46**, 2736–2738 (2010).
142. Tian, Z. et al. Highly sensitive and robust peroxidase-like activity of porous nanorods of ceria and their application for breast cancer detection. *Biomaterials* **59**, 116–124 (2015).
143. Asati, A., Santra, S., Kaittanis, C., Nath, S. & Perez, J. M. Oxidase-like activity of polymer-coated cerium oxide nanoparticles. *Angew. Chem. Int. Ed.* **121**, 2344–2348 (2009).
144. Vernekar, A. A., Das, T. & Mugesh, G. Vacancy-engineered nanoceria: enzyme mimetic hotspots for the degradation of nerve agents. *Angew. Chem. Int. Ed.* **55**, 1412–1416 (2016).
145. Kuchma, M. H. et al. Phosphate ester hydrolysis of biologically relevant molecules by cerium oxide nanoparticles. *Nanomedicine* **6**, 738–744 (2010).
146. Chen, Z. et al. Dual enzyme-like activities of iron oxide nanoparticles and their implication for diminishing cytotoxicity. *ACS Nano* **6**, 4001–4012 (2012). This article reports that iron oxide nanoparticles catalyze H_2O_2 with dual enzyme-like activities: peroxidase-like under acidic conditions producing hydroxyl radicals, and catalase-like under neutral conditions producing oxygen.
147. Fan, J. et al. Direct evidence for catalase and peroxidase activities of ferritin–platinum nanoparticles. *Biomaterials* **32**, 1611–1618 (2011).

148. Wang, Q. et al. Porous Co_3O_4 nanoplates with pH-switchable peroxidase- and catalase-like activity. *Nanoscale* **10**, 19140–19146 (2018).
149. Liang, H. et al. PEI-coated Prussian blue nanocubes as pH-switchable nanozyme: broad-pH-responsive immunoassay for illegal additive. *Biosens. Bioelectron.* **219**, 114797 (2023).
150. Feng, K. et al. Breaking the pH limitation of nanozymes: mechanisms, methods, and applications. *Adv. Mater.* **36**, 2401619 (2024).
151. Zhang, R., Fan, K. & Yan, X. In *Nanozymology: Connecting Biology and Nanotechnology* (ed Yan, X.) 279–329 (Springer Singapore, 2020).
152. Ma, Y., Tian, Z., Zhai, W. & Qu, Y. Insights on catalytic mechanism of CeO_2 as multiple nanozymes. *Nano Res.* **15**, 10328–10342 (2022).
153. Wang, Q. et al. A valence-engineered self-cascading antioxidant nanozyme for the therapy of inflammatory bowel disease. *Angew. Chem. Int. Ed.* **134**, e202201101 (2022).
154. Zhang, Y. et al. Integrating Pt nanoparticles with carbon nanodots to achieve robust cascade superoxide dismutase-catalase nanozyme for antioxidant therapy. *Nano Today* **49**, 101768 (2023).
155. Zhou, Q. et al. Cascaded nanozyme system with high reaction selectivity by substrate screening and channeling in a microfluidic device. *Angew. Chem. Int. Ed.* **61**, e202112453 (2022).
156. Liu, Y., Liu, L., Qu, Z., Yu, L. & Sun, Y. Supramolecular assembly of benzophenone alanine and copper presents high laccase-like activity for the degradation of phenolic pollutants. *J. Hazard. Mater.* **443**, 130198 (2023).
157. Chen, Y. et al. A manganese-based metal–organic framework as a cold-adapted nanozyme. *Adv. Mater.* **36**, 2206421 (2024). This article reports a nanozyme with cold-adaptive catalytic properties, maintaining stable peroxidase-like activity from 0 °C to 45 °C.
158. Xu, F. Oxidation of phenols, anilines, and benzenethiols by fungal laccases: correlation between activity and redox potentials as well as halide inhibition. *Biochemistry* **35**, 7608–7614 (1996).
159. Wang, J. et al. Construction of a bioinspired laccase-mimicking nanozyme for the degradation and detection of phenolic pollutants. *Appl. Catal. B* **254**, 452–462 (2019).
160. Wang, J., Huang, R., Qi, W., Su, R. & He, Z. Construction of biomimetic nanozyme with high laccase- and catecholase-like activity for oxidation and detection of phenolic compounds. *J. Hazard. Mater.* **429**, 128404 (2022).
161. Liang, H. et al. Multicopper laccase mimicking nanozymes with nucleotides as ligands. *ACS Appl. Mater. Interfaces* **9**, 1352–1360 (2017).
162. Maity, T., Jain, S., Solra, M., Barman, S. & Rana, S. Robust and reusable laccase mimetic copper oxide nanozyme for phenolic oxidation and biosensing. *ACS Sustain. Chem. Eng.* **10**, 1398–1407 (2022).
163. Bao, W., Tian, L., Wang, H., Tang, A. & Yang, H. Breaking through the pH limitation of $Fe_{1-x}S$ nanozymes using component-modulated coupled nanoclay. *Inorg. Chem.* **63**, 3366–3375 (2024).
164. Gao, Z., Xu, M., Hou, L., Chen, G. & Tang, D. Irregular-shaped platinum nanoparticles as peroxidase mimics for highly efficient colorimetric immunoassay. *Anal. Chim. Acta* **776**, 79–86 (2013).
165. Mao, Z. et al. Copper metal organic framework as natural oxidase mimic for effective killing of Gram-negative and Gram-positive bacteria. *Nanoscale* **14**, 9474–9484 (2022).
166. Wang, H. et al. Pyrrolic nitrogen dominated the carbon dot mimic oxidase activity. *Carbon* **179**, 692–700 (2021).
167. Ye, Z. et al. Preparation of two-dimensional Pd@Ir nanosheets and application in bacterial infection treatment by the generation of reactive oxygen species. *ACS Appl. Mater. Interfaces* **14**, 23194–23205 (2022).
168. Zhang, W. et al. Prussian blue nanoparticles as multienzyme mimetics and reactive oxygen species scavengers. *J. Am. Chem. Soc.* **138**, 5860–5865 (2016).
169. Su, L. et al. One-step analysis of glucose and acetylcholine in water based on the intrinsic peroxidase-like activity of Ni/Co LDHs microspheres. *J. Mater. Chem. B* **5**, 116–122 (2017).
170. Singh, S. et al. A phosphate-dependent shift in redox state of cerium oxide nanoparticles and its effects on catalytic properties. *Biomaterials* **32**, 6745–6753 (2011).
171. Mo, W.-C. et al. Reversible inhibition of iron oxide nanozyme by guanidine chloride. *Front. Chem.* **8**, 491 (2020).
172. Long, Y. J. et al. Visual observation of the mercury-stimulated peroxidase mimetic activity of gold nanoparticles. *Chem. Commun.* **47**, 11939–11941 (2011).
173. Vallabani, N. V. S., Karakoti, A. S. & Singh, S. ATP-mediated intrinsic peroxidase-like activity of Fe_3O_4-based nanozyme: one step detection of blood glucose at physiological pH. *Colloids Surf. B* **153**, 52–60 (2017).
174. Luo, W. et al. Self-catalyzed, self-limiting growth of glucose oxidase-mimicking gold nanoparticles. *ACS Nano* **4**, 7451–7458 (2010).
175. Mu, J., Zhang, L., Zhao, M. & Wang, Y. Co_3O_4 nanoparticles as an efficient catalase mimic: properties, mechanism and its electrocatalytic sensing application for hydrogen peroxide. *J. Mol. Catal. A Chem.* **378**, 30–37 (2013).
176. Xiong, X. et al. High carbonization temperature to trigger enzyme mimicking activities of silk-derived nanosheets. *Small* **16**, 2004129 (2020).
177. Liu, C. et al. NIR enhanced peroxidase-like activity of Au@CeO_2 hybrid nanozyme by plasmon-induced hot electrons and photothermal effect for bacteria killing. *Appl. Catal. B* **295**, 120317 (2021).
178. Zhu, Y. et al. Dual nanozyme-driven PtSn bimetallic nanoclusters for metal-enhanced tumor photothermal and catalytic therapy. *ACS Nano* **17**, 6833–6848 (2023).
179. Wu, H. et al. Enhanced tumor synergistic therapy by injectable magnetic hydrogel mediated generation of hyperthermia and highly toxic reactive oxygen species. *ACS Nano* **13**, 14013–14023 (2019).
180. Zhang, C. et al. X-ray-facilitated redox cycling of nanozyme possessing peroxidase-mimicking activity for reactive oxygen species-enhanced cancer therapy. *Biomaterials* **276**, 121023 (2021).
181. Zhu, X. et al. Engineering single-atom iron nanozymes with radiation-enhanced self-cascade catalysis and self-supplied H_2O_2 for radio-enzymatic therapy. *ACS Nano* **16**, 18849–18862 (2022).
182. Wang, L. et al. A molybdenum disulfide nanozyme with charge-enhanced activity for ultrasound-mediated cascade-catalytic tumor ferroptosis. *Angew. Chem. Int. Ed.* **62**, e202217448 (2023).
183. Yu, G.-H. et al. Fungal nanophase particles catalyze iron transformation for oxidative stress removal and iron acquisition. *Curr. Biol.* **30**, 2943–2950.e2944 (2020).
184. Chi, Z.-L., Yu, G.-H., Kappler, A., Liu, C.-Q. & Gadd, G. M. Fungal–mineral interactions modulating intrinsic peroxidase-like activity of iron nanoparticles: implications for the biogeochemical cycles of nutrient elements and attenuation of contaminants. *Environ. Sci. Technol.* **56**, 672–680 (2022).
185. Dai, S. et al. An inorganic mineral-based protocell with prebiotic radiation fitness. *Nat. Commun.* **14**, 7699 (2023).
186. Dai, S. et al. Dynamic polyphosphate metabolism coordinating with manganese ions defends against oxidative stress in the extreme bacterium deinococcus radiodurans. *Appl. Environ. Microbiol.* **87**, e02785–02720 (2021).
187. Akter, R. et al. Islet amyloid polypeptide: structure, function, and pathophysiology. *J. Diabetes Res.* **2016**, 2798269 (2016).

188. Chen, Y.-T., Hu, K.-W., Huang, B.-J., Lai, C.-H. & Tu, L.-H. Inhibiting human calcitonin fibril formation with its most relevant aggregation-resistant analog. *J. Phys. Chem. B* **123**, 10171–10180 (2019).
189. Xu, L. & Pu, J. Alpha-synuclein in Parkinson's disease: from pathogenetic dysfunction to potential clinical application. *Parkinson's Dis.* **2016**, 1720621 (2016).
190. Deng, H.-X. et al. Conversion to the amyotrophic lateral sclerosis phenotype is associated with intermolecular linked insoluble aggregates of SOD1 in mitochondria. *Proc. Natl. Acad. Sci. USA* **103**, 7142–7147 (2006).
191. Attar, F. et al. Nanozymes with intrinsic peroxidase-like activities. *J. Mol. Liq.* **278**, 130–144 (2019).
192. Singh, N., Sherin, G. R. & Mugesh, G. Antioxidant and prooxidant nanozymes: from cellular redox regulation to next-generation therapeutics. *Angew. Chem. Int. Ed.* **62**, e202301232 (2023).
193. Zhou, C., Wang, Q., Cao, H., Jiang, J. & Gao, L. Nanozybiotics: advancing antimicrobial strategies through biomimetic mechanisms. *Adv. Mater.* **36**, 2403362 (2024).
194. Xu, R. et al. Nanozyme-based strategies for efficient theranostics of brain diseases. *Coord. Chem. Rev.* **501**, 215519 (2024).
195. Giraldo, J. P. et al. Plant nanobionics approach to augment photosynthesis and biochemical sensing. *Nat. Mater.* **13**, 400–408 (2014).
196. Wu, H., Shabala, L., Shabala, S. & Giraldo, J. P. Hydroxyl radical scavenging by cerium oxide nanoparticles improves Arabidopsis salinity tolerance by enhancing leaf mesophyll potassium retention. *Environ. Sci. Nano* **5**, 1567–1583 (2018).
197. Xi, Z. et al. Nickel-platinum nanoparticles as peroxidase mimics with a record high catalytic efficiency. *J. Am. Chem. Soc.* **143**, 2660–2664 (2021).
198. Xu, R. et al. Norepinephrine-induced AuPd aerogels with peroxidase- and glucose oxidase-like activity for colorimetric determination of glucose. *Microchim. Acta* **188**, 362 (2021).
199. Zhang, H., Liang, X., Han, L. & Li, F. "Non-naked" gold with glucose oxidase-like activity: a nanozyme for tandem catalysis. *Small* **14**, 1803256 (2018).
200. Cong, C. et al. Dual-activity nanozyme to initiate tandem catalysis for doubly enhancing ATP-depletion anti-tumor therapy. *Biomater. Adv.* **143**, 213181 (2022).
201. Yao, J. et al. ROS scavenging Mn_3O_4 nanozymes for in vivo anti-inflammation. *Chem. Sci.* **9**, 2927–2933 (2018).
202. Mohammed Ameen, S. S. & Omer, K. M. Temperature-resilient and sustainable Mn-MOF oxidase-like nanozyme (UoZ-4) for total antioxidant capacity sensing in some citrus fruits: Breaking the temperature barrier. *Food Chem.* **448**, 139170 (2024).
203. Qin, T. et al. Low-temperature adaptive single-atom iron nanozymes against viruses in the cold chain. *Adv. Mater.* **36**, 2309669 (2024).
204. Fan, K. L. et al. Magnetoferritin nanoparticles for targeting and visualizing tumour tissues. *Nat. Nanotechnol.* **7**, 459–464 (2012).
205. Loynachan, C. N. et al. Renal clearable catalytic gold nanoclusters for in vivo disease monitoring. *Nat. Nanotechnol.* **14**, 883–890 (2019). This article reports an in vivo nanosensor combining Au nanoclusters with neutravidin, using the peroxidase-like activity of Au nanoclusters to enable early colorectal cancer diagnosis via colorimetric detection in mouse urine.
206. Hu, Y. et al. Surface-enhanced Raman scattering active gold nanoparticles with enzyme-mimicking activities for measuring glucose and lactate in living tissues. *ACS Nano* **11**, 5558–5566 (2017).
207. Li, Y., Li, P., Chen, Y., Wu, Y. & Wei, J. Interfacial deposition of Ag nanozyme on metal-polyphenol nanosphere for SERS detection of cellular glutathione. *Biosens. Bioelectron.* **228**, 115200 (2023).
208. Chen, Y. et al. Bifunctional Mo_2N nanoparticles with nanozyme and SERS activity: a versatile platform for sensitive detection of biomarkers in serum samples. *Anal. Chem.* **96**, 2998–3007 (2024).
209. Ren, X., Liu, J., Ren, J., Tang, F. & Meng, X. One-pot synthesis of active copper-containing carbon dots with laccase-like activities. *Nanoscale* **7**, 19641–19646 (2015).
210. Feng, L. et al. Iridium nanocrystals encapsulated liposomes as near-infrared light controllable nanozymes for enhanced cancer radiotherapy. *Biomaterials* **181**, 81–91 (2018).
211. Xi, J. et al. Light-enhanced sponge-like carbon nanozyme used for synergetic antibacterial therapy. *Biomater. Sci.* **7**, 4131–4141 (2019).
212. Dong, C. et al. A calcium fluoride nanozyme for ultrasound-amplified and Ca^{2+}-overload-enhanced catalytic tumor nanotherapy. *Adv. Mater.* **34**, 2205680 (2022).
213. Zhang, Y. et al. Genetically engineered magnetic nanocages for cancer magneto-catalytic theranostics. *Nat. Commun.* **11**, 5421 (2020).
214. Da, Y. et al. Advanced characterization techniques for identifying the key active sites of gas-involved electrocatalysts. *Adv. Funct. Mater.* **30**, 2001704 (2020).
215. Fan, Z. et al. In situ transmission electron microscopy for energy materials and devices. *Adv. Mater.* **31**, 1900608 (2019).
216. Cao, S. et al. A library of ROS-catalytic metalloenzyme mimics with atomic metal centers. *Adv. Mater.* **34**, 2200255 (2022).
217. Xu, Y. et al. The Fe-N-C nanozyme with both accelerated and inhibited biocatalytic activities capable of accessing drug–drug interactions. *Angew. Chem. Int. Ed.* **59**, 14498–14503 (2020).
218. Zhu, C. et al. Cascade nanozymatic network mimicking cells with selective and linear perception of H_2O_2. *Chem. Sci.* **14**, 6780–6791 (2023).
219. Su, J. et al. Single-site iron-anchored amyloid hydrogels as catalytic platforms for alcohol detoxification. *Nat. Nanotechnol.* **19**, 1168–1177 (2024). This article reports a biomimetic nanozyme hydrogel based on β-lactoglobulin fibrils with single-site iron anchors, mimicking horseradish peroxidase to catalyze alcohol oxidation and enable alcohol detoxification in vivo.
220. Wang, Z. et al. Accelerated discovery of superoxide-dismutase nanozymes via high-throughput computational screening. *Nat. Commun.* **12**, 6866 (2021).
221. Zhuang, J. et al. Machine-learning-assisted nanozyme design: lessons from materials and engineered enzymes. *Adv. Mater.* **36**, 2210848 (2024).
222. Li, Y., Zhang, R., Yan, X. & Fan, K. Machine learning facilitating the rational design of nanozymes. *J. Mater. Chem. B* **11**, 6466–6477 (2023).
223. Yu, Y. et al. Machine learning assisted graphdiyne-based nanozyme discovery. *ACS Mater. Lett.* **4**, 2134–2142 (2022).
224. Jiang, W. et al. Chiral metal-organic frameworks incorporating nanozymes as neuroinflammation inhibitors for managing Parkinson's disease. *Nat. Commun.* **14**, 8137 (2023).
225. Shen, X. et al. Nano-decocted ferrous polysulfide coordinates ferroptosis-like death in bacteria for anti-infection therapy. *Nano Today* **35**, 100981 (2020).
226. Cao, M. et al. In situ label-free X-ray imaging for visualizing the localization of nanomedicines and subcellular architecture in intact single cells. *Nat. Protoc.* **19**, 30–59 (2024).
227. Baimanov, D. et al. In situ analysis of nanoparticle soft corona and dynamic evolution. *Nat. Commun.* **13**, 5389 (2022).
228. Zhang, J., Ma, X. & Wang, Z. Surface-enhanced Raman scattering-fluorescence dual-mode nanosensors for quantitative detection of cytochrome c in living cells. *Anal. Chem.* **91**, 6600–6607 (2019).
229. Hughes, G. & Lewis, J. C. Introduction: biocatalysis in industry. *Chem. Rev.* **118**, 1–3 (2018).

230. Bommarius, A. S. & Paye, M. F. Stabilizing biocatalysts. *Chem. Soc. Rev.* **42**, 6534–6565 (2013).
231. Hudlicky, T. & Reed, J. W. Applications of biotransformations and biocatalysis to complexity generation in organic synthesis. *Chem. Soc. Rev.* **38**, 3117–3132 (2009).
232. Nel, A. E. et al. Understanding biophysicochemical interactions at the nano–bio interface. *Nat. Mater.* **8**, 543–557 (2009).
233. Roth, J. P. & Klinman, J. P. Catalysis of electron transfer during activation of O_2 by the flavoprotein glucose oxidase. *Proc. Natl. Acad. Sci.* **100**, 62–67 (2003).
234. Chen, J. et al. Glucose-oxidase like catalytic mechanism of noble metal nanozymes. *Nat. Commun.* **12**, 3375 (2021). This article reports that noble metal nanozymes catalyze glucose oxidation via a dehydrogenation mechanism, mimicking glucose oxidase activity.
235. Li-Zeng, G. & Xi-Yun, Y. Discovery and current application of nanozyme. *Prog. Biochem. Biophys.* **40**, 892–902 (2013).
236. Wang, D., Jana, D. & Zhao, Y. Metal–organic framework derived nanozymes in biomedicine. *Acc. Chem. Res.* **53**, 1389–1400 (2020).
237. Liu, Q. et al. Cofactor-free oxidase-mimetic nanomaterials from self-assembled histidine-rich peptides. *Nat. Mater.* **20**, 395–402 (2021). This article reports that the nanomaterials formed by self-assembly of polyhistidine peptides showed the activity of catalyzing the reduction of H_2O_2 in the absence of heme cofactors or metals.
238. He, S. et al. Osmium nanozyme as peroxidase mimic with high performance and negligible interference of O_2. *J. Mater. Chem. A* **8**, 25226–25234 (2020).
239. Meng, X. et al. Ultrasmall metal alloy nanozymes mimicking neutrophil enzymatic cascades for tumor catalytic therapy. *Nat. Commun.* **15**, 1626 (2024).
240. Sozarukova, M. M., Proskurnina, E. V., Popov, A. L., Kalinkin, A. L. & Ivanov, V. K. New facets of nanozyme activity of ceria: lipo- and phospholipoperoxidase-like behaviour of CeO_2 nanoparticles. *RSC Adv.* **11**, 35351–35360 (2021).
241. Wang, T., Su, P., Li, H., Yang, Y. & Yang, Y. Triple-enzyme mimetic activity of Co_3O_4 nanotubes and their applications in colorimetric sensing of glutathione. *New J. Chem.* **40**, 10056–10063 (2016).
242. Cao, C. et al. Starvation, ferroptosis, and prodrug therapy synergistically enabled by a cytochrome c oxidase like nanozyme. *Adv. Mater.* **34**, 2203236 (2022).
243. Chen, M. et al. Mimicking a natural enzyme system: cytochrome c oxidase-like activity of Cu_2O nanoparticles by receiving electrons from cytochrome c. *Inorg. Chem.* **56**, 9400–9403 (2017).
244. Guan, L. et al. Bioinspired Cu-based metal-organic framework mimicking SOD for superoxide anion sensing and scavenging. *Talanta* **265**, 124860 (2023).
245. Sun, M. et al. Site-selective photoinduced cleavage and profiling of DNA by chiral semiconductor nanoparticles. *Nat. Chem.* **10**, 821–830 (2018). This article reports that chiral cysteine-modified CdTe nanoparticles selectively cleave double-stranded DNA at the GAT'ATC restriction site upon photonic excitation, mimicking a restriction endonuclease.
246. Chen, D. et al. Magnetic $CuFe_2O_4$ with intrinsic protease-like activitycc inhibited cancer cell proliferation and migration through mediating intracellular proteins. *Biomater. Biosyst.* **5**, 100038 (2022).
247. Wang, F. et al. A biocompatible heterogeneous MOF–Cu catalyst for in vivo drug synthesis in targeted subcellular organelles. *Angew. Chem. Int. Ed.* **58**, 6987–6992 (2019).
248. Tao, G. et al. A strategy of local hydrogen capture and catalytic hydrogenation for enhanced therapy of chronic liver diseases. *Theranostics* **13**, 2455–2470 (2023).

Acknowledgements

This work was financially supported by the National Natural Science Foundation of China (Grant No. 81930050, X.Y.; 82122037, K.F.; 22121003, X.Y.; U23A20686, K.F.; 32301164, R.Z.), National Key Research and Development Program of China (No. 2021YFC2102900, K.F.; 2022YFA1205801, X.Y.), CAS Project for Young Scientists in Basic Research (YSBR-089, K.F.), Project supported by the Space Application System of China Manned Space Program (KJZ-YY-WSM0502, X.Y.), and Key Laboratory of Biomacromolecules, Chinese Academy of Sciences (ZGD-2023-03, K.F.).

Author contributions

K.F. and L.G. conceived the idea of the review and planned the outline. R.Z. researched the literature and wrote the draft under the supervision of K.F. and L.G., and K.F., L.G., and X.Y. revised the manuscript. All authors contributed to the discussion, editing, and finalizing of the content.

Competing interests

The authors declare no competing interests.

Additional information

Correspondence and requests for materials should be addressed to Lizeng Gao or Kelong Fan.

Peer review information *Nature Communications* thanks Yuanjian Zhang and the other, anonymous, reviewers for their contribution to the peer review of this work.